Electrical Double Layer Interaction between Dissimilar Spherical Colloidal Particles and between a Sphere and a Plate: The Linearized Poisson–Boltzmann Theory

Steven L. Carnie,* Derek Y. C. Chan, and James S. Gunning

Department of Mathematics, University of Melbourne, Parkville, Victoria 3052, Australia

Received March 14, 1994[⊗]

The linearized Poisson–Boltzmann theory is used to calculate the electrical double layer interaction free energy, as well as the double layer force, between unequal spherical colloidal particles. Results are given for interaction under conditions of constant surface potential, for constant surface charge, and for the case in which charge regulation due to the dissociation of surface groups may be modeled by a linear relationship between the surface charge and the surface potential. The interaction energy and force between a spherical colloidal particle and a plate, which has particular relevance to force measurements with the atomic force microscope and particle deposition studies, are also calculated. The results are used to test the accuracy of the linear Deryaguin approximation which forms the basis of the Hogg–Healy–Fuerstenau formula. The validity of the linearized Poisson–Boltzmann theory is tested against a numerical solution of the nonlinear Poisson–Boltzmann equation in the special case of spherical particles of the same size but opposite surface potentials.

I. Introduction

Although the fundamental theory for the electrical double layer interaction between colloidal particles has been established for more than half a century,[1,2] analytic expressions for the forces and free energies of interaction, even for spherical particles, are only available as approximate expressions such as the linear superposition approximation[3] (which is valid when the particles are far apart and the double layer overlap is relatively weak). Alternatively, one can use the Deryaguin construction (valid for thin double layers relative to the particle size) to derive the interaction free energy between spheres from that between parallel plates.[4] The advent of the atomic force microscope (AFM) has given colloid scientists the ability to measure directly the force between a colloidal particle and a planar surface.[5] In order to interpret such measurements, it would be useful to be able to compute the expected force curve, given parameters describing the colloidal particle and the surface. In this paper, we present results for the electrical double-layer force and interaction free energy, both for unequal spherical particles and for the sphere/plate geometry, based on the linearized Poisson–Boltzmann equation, but without any further restrictions regarding particle size, separation, and relative magnitudes of the surface potentials.

Part of the difficulty of calculating the force and interaction free energy is due to the nonlinear nature of the Poisson–Boltzmann theory which renders the problem analytically intractable except for the simplest geometries. However, in many practical problems, the surface potential of the particles are comparable to or only slightly larger than the thermal potential (kT/e). Conventionally, the linearized Poisson–Boltzmann theory is thought to be restricted to systems with electric potentials less than the thermal potential (kT/e), corresponding to about 25 mV at room temperature. Recent results for the force between two identical spherical colloidal particles using the nonlinear Poisson–Boltzmann theory[6] suggest that, in some circumstances, the linearized Poisson–Boltzmann equation gives fairly accurate results for potentials up to about 40 mV, that is, the region of applicability of the linearized Poisson–Boltzmann equation is larger than is usually supposed. As a consequence, it is desirable to have an accurate and convenient way to calculate the electrical double layer interaction based on the linearized Poisson–Boltzmann theory.

The theoretical framework for the analytic solution of the linearized Poisson–Boltzmann equation has been available for some time.[7] In this paper we provide an efficient method for calculating the double layer interaction free energy and force between two dissimilar spherical colloidal particles by solving the linearized Poisson–Boltzmann equation using a two center expansion method. Here we consider (a) particles which maintain a uniform fixed surface potential during interaction, the constant potential model, (b) particles that maintain a uniform fixed surface charge density during interaction, the constant charge model, and (c) particles that, as a result of the chemical ionization of surface groups, maintain a known relation between the surface potential and surface charge, the regulation model. For this last model, the surface charge-potential relationship is in general nonlinear for amphoteric or zwitterionic surfaces. This nonlinearity is inconsistent with the linearized Poisson–Boltzmann theory. However, we have shown elsewhere[8] that under appropriate conditions, it is possible to replace this charge-potential relation by a *linear* equation between the surface charge and the surface potential so that the method of solution for the cases of constant potential and constant charge models can be readily extended to the linearized regulation model to calculate the interaction free energy and force.

Previous work for identical spherical particles has used the two center expansion method to calculate the force

[⊗] Abstract published in *Advance ACS Abstracts,* July 15, 1994.

(1) Verwey, E. J. W.; Overbeek, J. Th. G. *Theory of the Stability of Lyophobic Colloids*; Elsevier: New York, 1948.

(2) Deryaguin, B. V.; Landau, L. D. *Acta Phys.-Chim. USSR* **1941**, *14*, 633.

(3) Bell, G. M.; Levine, S.; McCartney, L. N. *J. Colloid Interface Sci.* **1970**, *33*, 335.

(4) Hogg, R.; Healy, T. W.; Fuerstaneau, D. W. *Trans. Faraday Soc.* **1966**, *62*, 1638.

(5) Ducker, W. A.; Senden, T. J.; Pashley, R. M. *Nature* **1991**, *353*, 239.

(6) Carnie, S. L.; Chan, D. Y. C.; Stankovich, J. *J. Colloid Interface Sci.* **1994**, *165*, 116.

(7) Glendinning, A. B.; Russel, W. B. *J. Colloid Interface Sci.* **1983**, *93*, 95.

(8) Carnie, S. L.; Chan, D. Y. C. *J. Colloid Interface Sci.* **1993**, *161*, 260.

0743-7463/94/2410-2993$04.50/0

between the particles for the constant potential and constant charge models[7] and the linearized regulation model[9] and the interaction free energy for all the above surface models.[10,11] The only similar work we are aware of for unequal spheres obtained the force for spheres at constant potential and then integrated numerically to obtain the interaction free energy.[12] Ohshima has recently obtained an explicit (albeit involved) analytic series solution for the interaction free energy for unequal spheres at constant potential.[13] We are unaware of any previous work in the sphere/plate geometry.

In our previous work on identical spheres,[10] we allowed for the possibility of the particles having arbitrary dielectric constant ϵ_p which is relevant to cases b and c described above. For the common case $\epsilon_p < 5$ in a highly polar solvent, the energy and force are well approximated by those for $\epsilon_p = 0$ (for an illustration of this, see ref 6), and so we follow this simplification here. The more general case can be dealt with using the methods in ref 10, if desired.

Our method of solving the lineraized Poisson–Boltzmann equation for the electrostatic potential near two interacting spheres is based on a two center expansion in terms of spherical harmonics. The coefficients in this expansion are found by solving a system of linear equations that arise from matching boundary conditions at the particle surfaces. In section II, we derive this system of linear equations for various combinations of boundary conditions on each interacting spheres. In sections III and IV, we give the formulas for the force and interaction free energy in terms of the expansion coefficients. For the interaction between a sphere and a plate, a slightly different expansion for the electrostatic potential is required. This is because the series expansion of the potential around two spheres ceases to converge as the radius of one sphere goes to infinity to form a plate. In section V, we furnish this new expansion for the electrostatic potential for the interaction between a sphere and a plate and derive the system of equations that has to be solved to find the coefficients of this expansion. Expressions for the force and interaction free energy are given in sections VI and VII for the sphere/plate interaction. Numerical results are presented in section VIII and conclusions in section IX.

II. The Potential around Interacting Dissimilar Spheres

We now outline the method of determining the electrostatic potential near the two interacting spheres. In the linearized Poisson–Boltzmann model the electrostatic potential ψ satisfies the equation

$$\nabla^2 \psi = \kappa^2 \psi \qquad \text{(outside the spheres)} \qquad (1)$$

in the electrolyte characterized by κ, the inverse Debye length. With the assumption of zero dielectric constant for the particles, $\epsilon_p = 0$, it is only necessary to determine the potential in the region exterior to the spheres. We set up a coordinate system with the origin located midway between the centers of the spheres of radius a_1 and a_2, as shown in Figure 1.

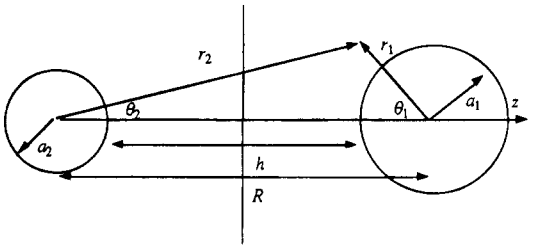

Figure 1. Coordinate system for two dissimilar spheres.

In the electrolyte ($r_1 > a_1$ and $r_2 > a_2$), the solution of (1) can be written as a two center expansion using spherical harmonics[7]

$$\psi = \sum_{n=0}^{\infty}\{a_n k_n(\kappa r_1)P_n(\cos\theta_1) + b_n k_n(\kappa r_2)P_n(\cos\theta_2)\}$$

$$= \sum_{n=0}^{\infty}\{a_n k_n(\kappa r_1)P_n(\cos\theta_1) + b_n \sum_{m=0}^{\infty}(2m+1)\times B_{nm}\, i_m(\kappa r_1)P_m(\cos\theta_1)\}$$

$$= \sum_{n=0}^{\infty}\{b_n k_n(\kappa r_2)P_n(\cos\theta_2) + a_n \sum_{m=0}^{\infty}(2m+1)\times B_{nm}\, i_m(\kappa r_2)P_m(\cos\theta_2)\} \quad (2)$$

where

$$B_{nm} = \sum_{\nu=0}^{\infty} A^{\nu}_{nm}\, k_{n+m-2\nu}(\kappa R) \qquad (3)$$

$$A^{\nu}_{nm} = \Gamma\left(n-\nu+\frac{1}{2}\right)\Gamma\left(m-\nu+\frac{1}{2}\right)\Gamma\left(\nu+\frac{1}{2}\right)\times (n+m-\nu)!\left(n+m-2\nu+\frac{1}{2}\right)\Big/\pi\,\Gamma\left(m+n-\nu+\frac{3}{2}\right)\times (n-\nu)!\,(m-\nu)!\,\nu! \quad (4)$$

The distance between the centers of the two spheres is R, $\Gamma(z)$ is the Gamma function, $P_n(x)$ is a Legendre polynomial of order n, and $i_n(x)$ and $k_n(x)$ are, respectively, modified spherical Bessel functions of the first and third kind[14] and are related to modified Bessel function of half integer order $I_{n+1/2}(x)$ and $K_{n+1/2}(x)$ by $i_n(x) = (\pi/2x)^{1/2}I_{n+1/2}(x)$ and $k_n(x) = (\pi/2x)^{1/2}K_{n+1/2}(x)$.

The unknown coefficients $\{a_n\}$ and $\{b_n\}$ are found by applying the appropriate boundary conditions on the surfaces of the spheres. We now give in detail the equations that need to be solved to find the coefficients. It will become clear that the constant charge model is actually a special case of the linearized regulation model. Since the two spheres are not forced to have the same surface model, this means we have three distinct cases—each sphere can have either constant potential or linearized regulation boundary conditions: (a) constant surface potential model on both spheres; (b) constant potential on one sphere and linearized regulation or constant charge on the other; (c) both spheres with linearized regulation boundary conditions. The constant charge boundary condition is a special limit of the linearized regulation boundary condition. We now give the equations that are needed to solve for the unknown coefficients $\{a_n\}$ and $\{b_n\}$ that appear in the spherical harmonic expansion for the electrostatic potential in eq 2 for the three cases listed.

(9) Krozel, J. W.; Saville, D. A. *J. Colloid Interface Sci.* **1992**, *150*, 365.
(10) Carnie, S. L.; Chan, D. Y. C. *J. Colloid Interface Sci.* **1993**, *155*, 297.
(11) Reiner, E. S.; Radke, C. J. *Adv. Colloid Interface Sci.* **1993**, *47*, 59.
(12) Kim, S.; Zukowski, C. F. *J. Colloid Interface Sci.* **1990**, *139*, 198.
(13) Ohshima, H. *J. Colloid Interface Sci.* **1994**, *162*, 487.
(14) Abramowitz, M.; Stegun, I. A. *Handbook of Mathematical Functions*; Dover: New York, 1965.

(a) Constant Surface Potential Model on Both Spheres. When the potential on the surface of both spheres is uniform and remains fixed at ψ_1 and ψ_2, respectively, the coefficients a_n and b_n can be found by applying the condition $\psi = \psi_1$ at $r_1 = a_1$ and $\psi = \psi_2$ at $r_2 = a_2$. Using eqs 2–4 this gives a system of linear equations

$$\mathbf{Ia} + \mathbf{Lb} = \psi_1 \mathbf{e} \tag{5a}$$

$$\mathbf{Ma} + \mathbf{Ib} = \psi_2 \mathbf{e} \tag{5b}$$

where the components of the vector of coefficients are given by

$$\mathbf{a}_j = a_j k_j(\kappa a_1) \tag{6a}$$

$$\mathbf{b}_j = b_j k_j(\kappa a_2) \tag{6b}$$

the matrix elements of **L** and **M** are

$$\mathbf{L}_{jn} = (2j+1) B_{nj} i_j(\kappa a_1)/k_n(\kappa a_2) \tag{7a}$$

$$\mathbf{M}_{jn} = (2j+1) B_{nj} i_j(\kappa a_2)/k_n(\kappa a_1) \tag{7b}$$

and

$$\mathbf{e}_j = \begin{cases} 1, & j = 0 \\ 0, & j > 0 \end{cases} \tag{8a}$$

$$\mathbf{I}_{ij} = \begin{cases} 1, & j = i \\ 0, & j \neq i \end{cases} \tag{8b}$$

There should be no confusion between the coefficients $\{a_n\}$ and the radii a_1 and a_2. The coefficients always have generic subscripts.

It can easily be seen that, for the case of spheres of equal size and surface potential, we recover the previous results.[7] A system of equations for the coefficients $\{a_n\}$ and $\{b_n\}$ can also be obtained by collocating the first form of eq 2 at a set of points on the surface of each sphere, as done in ref 12. We have tried both methods—they give identical results and require about the same size matrices so there seems to be no pressing reason to choose one method over the other.

(b) Constant Potential on One Sphere and Linearized Regulation or Constant Charge on the Other. We can, without loss of generality, choose sphere 1 to have constant surface potential and sphere 2 to have the linearized regulating boundary condition. The most general form of a linear relation connecting the surface charge density, σ, and the surface potential, ψ, that models surface ionization is given by

$$\sigma = S - K\psi \tag{9}$$

where the sign of the constant S is the same as the sign of the surface charge when the particle is in isolation. The constant K is always positive: its magnitude reflects the ability of the surface ionization reactions to maintain a constant surface charge. The limit $K = 0$ corresponds to a constant charge surface. For later reference, we call the constant K, the *regulation capacity* since it has the dimension of electrostatic capacitance per unit area (F/m^2). Previously,[10] we used the symbols K_1 and K_2 for S and K, respectively; here, for obvious reasons, we reserve the subscripts 1 and 2 to refer to the spheres.

For the case $\epsilon_p = 0$, the surface charge satisfies the equation

$$\sigma = -\epsilon \nabla\psi \cdot \mathbf{n} \qquad \text{at } r_1 = a_1 \text{ or } r_2 = a_2 \tag{10}$$

where $\epsilon = \epsilon_0 \epsilon_r$ is the product of the permittivity of free space, ϵ_0, and the relative permittivity of the solvent, ϵ_r, and **n** is the outward surface normal.

Applying the boundary conditions (9) together with (10) at $r_2 = a_2$ and setting $\psi = \psi_1$ at $r_1 = a_1$, we obtain the system of linear equations for the coefficients $\{a_n\}$ and $\{b_n\}$

$$\mathbf{Ia} + \mathbf{Lb} = \psi_1 \mathbf{e} \tag{11a}$$

$$\mathbf{Ma} + \mathbf{Ib} = \frac{a_2 S_2}{\epsilon}\mathbf{e} = \psi_2 \left(1 + \kappa a_2 + \frac{a_2 K_2}{\epsilon}\right)\mathbf{e} \tag{11b}$$

where

$$\mathbf{a}_j = a_j k_j(\kappa a_1) \tag{12a}$$

$$\mathbf{b}_j = [(a_2 K_2/\epsilon) k_j(\kappa a_2) - \kappa a_2 k'_j(\kappa a_2)] b_j \tag{12b}$$

$$\mathbf{L}_{jn} = (2j+1) B_{nj} i_j(\kappa a_1)/[(a_2 K_2/\epsilon) k_n(\kappa a_2) - \kappa a_2 k'_n(\kappa a_2)] \tag{12c}$$

$$\mathbf{M}_{jn} = (2j+1) B_{nj} [(a_2 K_2/\epsilon) i_j(\kappa a_2) - \kappa a_2 i'_j(\kappa a_2)]/k_n(\kappa a_1) \tag{12d}$$

In the second equality of eq 11b, we have eliminated the quantity S_2 in favor of the surface potential of sphere 2 when it is in isolation, ψ_2, and the regulation capacity of sphere 2, K_2.

The case in which sphere 2 has a constant charge boundary condition can be obtained by taking the limit $K_2 \to 0$.

(c) Both Spheres with Linearized Regulation Boundary Conditions. Applying the boundary conditions 9 and 10 on the surfaces of both spheres, we obtain the system of linear equations for the coefficients $\{a_n\}$ and $\{b_n\}$

$$\mathbf{Ia} + \mathbf{Lb} = \psi_1 \left(1 + \kappa a_1 + \frac{a_1 K_1}{\epsilon}\right)\mathbf{e} \tag{13a}$$

$$\mathbf{Ma} + \mathbf{Ib} = \psi_2 \left(1 + \kappa a_2 + \frac{a_2 K_2}{\epsilon}\right)\mathbf{e} \tag{13b}$$

where

$$\mathbf{a}_j = [(a_1 K_1/\epsilon) k_j(\kappa a_1) - \kappa a_1 k'_j(\kappa a_1)] a_j \tag{14a}$$

$$\mathbf{b}_j = [(a_2 K_2/\epsilon) k_j(\kappa a_2) - \kappa a_2 k'_j(\kappa a_2)] b_j \tag{14b}$$

$$\mathbf{L}_{jn} = (2j+1) B_{nj} \frac{(a_1 K_1/\epsilon) i_j(\kappa a_1) - \kappa a_1 i'_j(\kappa a_1)}{(a_2 K_2/\epsilon) k_n(\kappa a_2) - \kappa a_2 k'_n(\kappa a_2)} \tag{15a}$$

$$\mathbf{M}_{jn} = (2j+1) B_{nj} \frac{(a_2 K_2/\epsilon) i_j(\kappa a_2) - \kappa a_2 i'_j(\kappa a_2)}{(a_1 K_1/\epsilon) k_n(ka_1) - \kappa a_1 k'_n(\kappa a_1)} \tag{15b}$$

and ψ_1 and ψ_2 are the surface potentials of the spheres when they are infinitey far apart.

For each of the cases where the surface is modeled with linearized regulation equations, the special case of a constant charge surface can be obtained by simply setting the appropriate value of K to zero.

Provided $R > (a_1 + a_2)$, the coefficients of the exterior solution $\{a_n\}$ and $\{b_n\}$ are then found by truncating the matrix equations (5, 11, or 13) at an appropriate upper limit and solving the system of equations by direct numerical methods. We defer discussion of the choice of the cutoff size of the system of linear equations until later in this paper. We now proceed to derive expressions for

the force and interaction free energy in terms of the coefficients $\{a_n\}$ and $\{b_n\}$ which appear in the spherical harmonic expansions of the potential outside the spheres as given by eq 2.

III. The Force between Dissimilar Spheres

We can calculate the force acting on the particles by integrating the stress tensor

$$\mathbf{T} = \left(\prod + \frac{1}{2}\epsilon \mathbf{E}^2\right)\mathbf{I} - \epsilon \mathbf{EE} \tag{16}$$

over a suitable surface. Here $\mathbf{E} = -\nabla\psi$ is the electric field and $\prod$ is the *difference* in the local osmotic pressure from that in the bulk electrolyte solution. In the linearized Poisson–Boltzmann theory this difference in osmotic pressure is related to the electrostatic potential by

$$\prod = \frac{1}{2}\epsilon\kappa^2\psi^2 \tag{17}$$

If we want to evaluate the force on sphere 2 (due to the presence of sphere 1), we can choose any convenient surface S that encloses sphere 2 and perform the following surface integral to get the vector force on sphere 2

$$\mathbf{f} = \int_S \mathbf{T}\cdot\mathbf{n}\, dS \tag{18}$$

where the unit normal $\mathbf{n}$ at the surface S is directed toward sphere 2. Here we calculate the force on sphere 2 by choosing S to be the surface of sphere 1 ($r_1 = a_1$) so that $\mathbf{n}$ will be the radius vector directed away from the center of sphere 1—the outward surface normal. By setting the origin of a Cartesian axis system at the center of sphere 1 and the z axis to lie along the line joining the center of the spheres, the *magnitude* of the force on sphere 2 in the z direction can be expressed as integrals over functions of the r and θ components of the electric field:

$$f = \mathbf{f}\cdot\mathbf{z} = 2\pi a_1^2\epsilon \int_{-1}^{1}\left\{\frac{1}{2}[\kappa^2\psi^2 + E_\theta^2 - E_r^2]\mu + E_\theta E_r(1-\mu^2)^{1/2}\right\} d\mu \tag{19}$$

where the integrand is evaluated on the *outside* surface of sphere 1 ($r_1 = a_1^+$) and the integration variable μ is $\mu = \cos\theta_1$. Positive values of f imply repulsion between the spheres.

The evaluation of eq 19 proceeds differently for (a) a constant potential sphere as compared to (b) a sphere with linearized regulation boundary conditions. We shall consider these two cases separately.

(a) Sphere 1 at Constant Surface Potential. For either the constant potential model or the case where sphere 1 is at constant surface potential and sphere 2 is a linearized regulating surface, eq 19 for the repulsive force between the particles simplifies to

$$f = -\pi a_1^2\epsilon\int_{-1}^{1} E_r^2\mu\, d\mu \tag{20}$$

If we write the potential from eq 2 in the form

$$\psi = \sum_{n=0}^{\infty} d_n(\kappa r_1)\, P_n(\cos\theta_1) \tag{21}$$

where

$$d_n(\kappa r_1) \equiv a_n k_n(\kappa r_1) + (2n+1) i_n(\kappa r_1)\sum_{m=0}^{\infty} b_m B_{mn} \tag{22}$$

then the force in eq 20 becomes

$$f = -\pi\epsilon(\kappa a_1)^2\sum_{n=0}^{\infty}\{d'_n(\kappa a_1)\sum_{p=0}^{\infty} d'_p(\kappa a_1) C_1(p,n)\} \tag{23}$$

where the functions d'_n and d'_p are the derivatives of d_n and d_p and

$$C_1(n,m) = \int_{-1}^{1}\mu P_n(\mu)P_m(\mu)\, d\mu = \begin{cases} \dfrac{2(m+1)}{(2m+3)(2m+1)}, & n = m+1 \\ \dfrac{2m}{(2m+1)(2m-1)}, & n = m-1 \\ 0, & n \neq m \pm 1 \end{cases} \tag{24}$$

In what follows we shall present results for a nondimensional force

$$F = \frac{f}{\epsilon(kT/e)^2} \tag{25}$$

i.e. we scale by the thermal potential rather than any of the particle surface potentials as was done previously[7,9,10] because we want to have the freedom to let either particle have zero surface potential. This means that

$$F = -\pi(\kappa a_1)^2\sum_{n=0}^{\infty}\{d'_n(\kappa a_1)\sum_{p=0}^{\infty} d'_p(\kappa a_1) C_1(p,n)\} \tag{26}$$

where the potentials appearing in the governing equations (5 or 11) are to be interpreted as $(e\psi/kT)$, that is, the potential scaled by the thermal potential.

(b) Sphere 1 a Linearized Regulating Surface. For the other two cases, eq 19 for the repulsive force between the particles can be rewritten, using $E_r = \sigma/\epsilon = (S_1 - K_1\psi)\epsilon$, as

$$f = \pi\epsilon\int_{-1}^{1}\left\{\left[(\kappa a_1)^2\psi^2 + (\partial\psi/\partial\mu)^2(1-\mu^2) + 2\left(\frac{a_1S_1}{\epsilon}\right)\times\left(\frac{a_1K_1}{\epsilon}\right)\psi - \left(\frac{a_1K_1}{\epsilon}\right)^2\psi^2\right]\mu + 2\left(\frac{\partial\psi}{\partial\mu}\right)\left(\frac{a_1S_1}{\epsilon}\right)(1-\mu^2) - 2\left(\frac{\partial\psi}{\partial\mu}\right)\left(\frac{a_1K_1}{\epsilon}\right)\psi(1-\mu^2)\right\} d\mu \tag{27}$$

Explicitly, the nondimensional force is

$$F = \pi\left\{\left(\frac{4}{3}\right)\left(\frac{a_1S_1}{\epsilon}\right)\left[\left(\frac{a_1K_1}{\epsilon}\right) + 2\right]d_1\right\} + \sum_{n=0}^{\infty}\left\{d_n(\kappa a_1)\sum_{p=0}^{\infty} d_p(\kappa a_1)\left[C_3(p,n) - 2\left(\frac{a_1K_1}{\epsilon}\right)C_2(p,n) + \left((\kappa a_1)^2 - \left(\frac{a_1K_1}{\epsilon}\right)^2\right)C_1(p,n)\right]\right\} \tag{28}$$

where

$$C_2(n,m) = \int_{-1}^{1}(1-\mu^2)P_n(\mu)P_m'(\mu)\, d\mu = \begin{cases} \dfrac{-2m(m+1)}{(2m+3)(2m+1)}, & n = m+1 \\ \dfrac{2m(m+1)}{(2m+1)(2m-1)}, & n = m-1 \\ 0, & n \neq m \pm 1 \end{cases} \tag{29}$$

$$C_3(n,m) = \int_{-1}^{1}\mu(1-\mu^2)P_n'(\mu)P_m'(\mu)d\mu = \begin{cases} \dfrac{2m(m+1)(m+2)}{(2m+3)(2m+1)}, & n = m+1 \\ \dfrac{2m(m-1)(m+1)}{(2m+1)(2m-1)}, & n = m-1 \\ 0, & n \neq m \pm 1 \end{cases} \quad (30)$$

Again, the quantity S_1 can be eliminated in favor of ψ_1 and K_1, see eq 11b. Thus having solved the set of linear equations given in section II for the coefficients $\{a_n\}$ and $\{b_n\}$, the results can be substituted into the above equations to calculate the force.

IV. The Interaction Free Energy between Dissimilar Spheres

While the expressions for the force between the particles are somewhat cumbersome, the expressions for the interaction free energy take on very simple forms. We calculate the interaction free energy for all cases by a thermodynamic integration otherwise known as a coupling constant integration or charging procedure. This scheme has a very simple graphical representation in terms of the surface charge–surface potential relationships.[1,8,15] For the linearized Poisson–Boltzmann model, the thermodynamic integrations are trivial. Furthermore, considerable simplification is afforded by judicious use of the $j = 0$ equation in the linear systems for the unknown coefficient a_n and b_n given in eqs 5, 11, or 13 to eliminate terms like $\Sigma a_n B_{n0}$.

The interaction free energy between the two spheres with a distance of closest approach $h = R - a_1 - a_2$ can be written as a sum of surface integrals over each sphere:

$$u(h) = u_1(h) + u_2(h) = (2\pi a_1^2)\int_{-1}^{1}u_1(h,\mu_1)\,d\mu_1 + (2\pi a_2^2)\int_{-1}^{1}u_2(h,\mu_2)\,d\mu_2 \quad (31)$$

The quantity $u_k(h,\mu)$ (with $k = 1, 2$) is the interaction free energy per unit area at position $\mu = \cos\theta$ on the surface of the sphere k when the spheres are at a distance h apart. The surface model for each sphere determines the appropriate expression for $u_1(h)$ and $u_2(h)$. We present details of the derivation of $u_1(h)$, the corresponding expression for $u_2(h)$ can be found by interchanging the indices $1 \leftrightarrow 2$ and exchanging for the appropriate coefficient as detailed below. There are two different forms for the integrands $u_1(h,\mu_1)$ and $u_2(h,\mu_2)$ depending on whether the constant potential or linearized regulation boundary condition applies at the sphere. The constant charge boundary condition is a special case of the linearized regulation boundary condition. We now derive expressions for $u_1(h,\mu_1)$ for these two different boundary conditions.

(a) Constant Surface Potential Sphere. The interaction free energy per unit area when the sphere is held at constant surface potential ψ_1 is given by

$$u_1(h,\mu) = -\int_0^{\psi_1}[\sigma(\psi,h,\mu) - \sigma(\psi,\infty,\mu)]\,d\psi \quad (32a)$$

$$= -\frac{1}{2}[\sigma(h,\mu) - \sigma(\infty,\mu)]\psi_1 \quad (32b)$$

where $\sigma(h,\mu)$ is the surface charge at $\mu = \cos\theta$ on sphere 1 when the spheres are at a separation h. While (32a) is general for constant surface potential interactions, (32b) is only valid for the linearized Poisson–Boltzmann model.

Using (10) and (21), we get

$$u_1(h) = 2\pi a_1^2\kappa\epsilon\psi_1\left[d'_0(\kappa a_1) - \psi_1\frac{k'_0(\kappa a_1)}{k_0(\kappa a_1)}\right] \quad (33)$$

where the second term comes from the contribution at $h = \infty$. Using the $j = 0$ equation in either (5a) or (11a), this simplifies to

$$U_1(h) = \frac{u_1(h)}{(\epsilon(kT/e)^2\kappa^{-1})} = 2\pi\psi_1\left[\psi_1\frac{\exp(\kappa a_1)}{\sinh(\kappa a_1)}(\kappa a_1)^2 - \frac{\pi a_0}{2i_0(\kappa a_1)}\right] \quad (34)$$

where U is the nondimensional energy

$$U(h) = \frac{u(h)}{(\epsilon(kT/e)^2\kappa^{-1})} \quad (35)$$

which again is different to our previous scaling.[10] As for the force, the potential ψ_1 in (34) for the nondimensional interaction free energy should be interpreted as potentials scaled by the thermal potential.

If sphere 2 has a constant surface potential, we simply change the subscripts in (34) from 1 to 2 and use b_0 in place of a_0.

(b) Linearized Regulation Sphere. The interaction free energy per unit area for a sphere with linearized regulation condition as a function of surface position $\mu = \cos\theta$ is given by[8]

$$u_1(h,\mu) = \frac{1}{2}[\psi(h,\mu) - \psi(\infty,\mu)]S_1 \quad (36)$$

where $\psi(h,\mu)$ is the surface potential at position $\mu = \cos\theta$ on the surface of the sphere when the spheres are at a distance h apart.

Using equation (21), we get

$$u_1(h) = 2\pi a_1^2 S_1 \times \left\{d_0(\kappa a_1) - \frac{a_1 S_1}{\epsilon}\frac{k'_0(\kappa a_1)}{\left[\frac{a_1 K_1}{\epsilon}k_0(\kappa a_1) - \kappa a_1 k'_0(\kappa a_1)\right]}\right\} \quad (37)$$

where again the second term comes from the contribution at $h = \infty$. Using the first equation ($j = 0$) in (13a) for the coefficient a_0, the nondimensional interaction free energy simplifies to

$$U_1(h) = 2\pi\kappa a_1\psi_1\left(1 + \kappa a_1 + \frac{a_1 K_1}{\epsilon}\right) \times \left\{\frac{k_0(\kappa a_1)}{\left[\frac{a_1 K_1}{\epsilon}k_0(\kappa a_1) - \kappa a_1 k'_0(\kappa a_1)\right]} - \frac{i_0(\kappa a_1)}{\left[\frac{a_1 K_1}{\epsilon}i_0(\kappa a_1) - \kappa a_1 i'_0(\kappa a_1)\right]}\right\}\left\{a_0\left[\frac{a_1 K_1}{\epsilon}k_0(\kappa a_1) - \kappa a_1 k'_0(\kappa a_1)\right] - \psi_1\left(1 + \kappa a_1 + \frac{a_1 K_1}{\epsilon}\right)\right\} \quad (38)$$

(15) Chan, D. Y. C. In *Geochemical Processes at Mineral Surfaces*; Davis, J. A., Hayes, K. F., Eds.; ACS Symposium Series No. 323; American Chemical Society: Washington, DC, 1986; p 99.

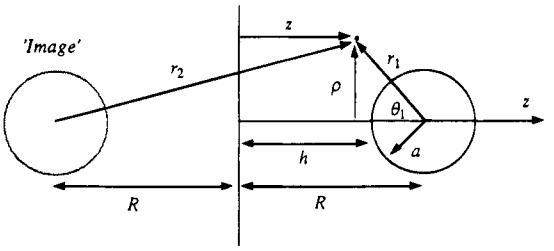

Figure 2. Coordinate system for a sphere and a plate.

where we have eliminated S_1 in terms of ψ_1, the potential of the sphere at infinite separation. The potential ψ_1 in eq 38 should be interpreted as the nondimensional potential ($e\psi/kT$). Again, if sphere 2 has a linearized regulating surface, U_2 can be found from (38) by changing subscripts from 1 to 2 and using b_0 in place of a_0. This completes the specification of the force and interaction free energy for unequal spheres.

V. The Potential in a Sphere/Plate Geometry

We now consider the solution of the electrostatic potential for the interaction between a sphere and a flat plate. The addition theorem for Bessel functions that lies at the heart of the potential representation in eq 2 becomes invalid in the case where one of the particle radii becomes infinite, that is, the sphere/plate geometry. This means we must look for an alternative representation for the potential.

In order to motivate our choice, first consider the case of a plate at constant zero surface charge. Near the sphere the potential is represented by the same expansion in $k_n(\kappa r_1)P_n(\cos\theta_1)$ as before. The electric field normal to the surface must be zero at the plate due to the zero surface charge boundary condition imposed. This condition can be maintained by placing an image sphere of the same properties at a position reflected in the plate, the center of the image sphere at a distance R behind the plate. Then the potential has the form

$$\psi = \sum_{n=0}^{\infty} a_n \{k_n(\kappa r_1)P_n(\cos\theta_1) + k_n(\kappa r_2)P_n(\cos\theta_2)\}$$

where the coordinates (r_1,θ_1), (ϱ,z), and (r_2,θ_2), as well as the distance R are defined in Figure 2. This representation for the potential satisfies the field equation outside the sphere and plate and satisfies the boundary condition at the plate. The coefficients $\{a_n\}$ are found by applying the appropriate boundary condition on the sphere, as done in section II. We now consider representations for the potential for the cases in which the plate obeys constant charge, constant potential, or linearized regulation boundary conditions.

If the surface charge on the plate $\sigma \neq 0$, we can add the term $\psi_0 e^{-\kappa z}$ to the potential. This additional term still satisfies the field equation, eq 1, and if we choose the constant $\psi_0 = (\sigma/\epsilon\kappa)$, the boundary condition on the plate, eq 10, will also be met. So for the case of a constant *charge* plate we have

$$\psi = \sum_{n=0}^{\infty} a_n\{k_n(\kappa r_1)P_n(\cos\theta_1) + k_n(\kappa r_2)P_n(\cos\theta_2)\} + (\sigma/\epsilon\kappa)e^{-\kappa z} \quad (39)$$

If the plate is at constant potential ψ_p instead of at constant charge, an image sphere with the same magnitude in the potential but opposite in sign will produce zero potential on the plate and the choice $\psi_0 = \psi_p$ will satisfy the boundary condition on the plate. So for the case of a constant *potential* plate we have

$$\psi = \sum_{n=0}^{\infty} a_n\{k_n(\kappa r_1)P_n(\cos\theta_1) - k_n(\kappa r_2)P_n(\cos\theta_2)\} + \psi_p e^{-\kappa z} \quad (40)$$

In the case where the plate obeys the linearized regulation boundary condition, we can use the following representation for the potential

$$\psi = \sum_{n=0}^{\infty} \{a_n k_n(\kappa r_1)P_n(\cos\theta_1) + b_n k_n(\kappa r_2)P_n(\cos\theta_2)\} + \psi_0 e^{-\kappa z} \quad (41)$$

where the constant ψ_0 is yet to be determined. In the special cases of constant charge plate and constant potential plate, we know

$$b_n = a_n \qquad \text{(constant charge plate)}$$

$$b_n = -a_n \qquad \text{(constant potential plate)} \quad (42)$$

as well as the value of the constant ψ_0. We use the special forms in eqs 39 and 40 when applicable since they halve the number of unknowns to solve for; in the most general case, we must use the form (41).

In all cases we must satisfy the appropriate boundary condition on the sphere. This is made possible by using the expansion[14]

$$e^{-\kappa z} = e^{-\kappa R}\, e^{-\kappa(z-R)} = e^{-\kappa R} \exp(\kappa r_1 \cos\theta_1)$$

$$= e^{-\kappa R} \sum_{n=0}^{\infty} (2n+1) i_n(\kappa r_1) P_n(\cos\theta_1) \quad (43)$$

to express $e^{-\kappa z}$ in terms of the coordinates centered about the sphere. We now give the equations that determine the coefficients $\{a_n\}$ and $\{b_n\}$ that arise from matching boundary conditions at the sphere. If the plate is held at constant charge or constant potential, we only have one set of unknown coefficients $\{a_n\}$ to determine, but if the plate obeys the linearized regulation boundary condition, we need to determine two sets of coefficients: $\{a_n\}$ and $\{b_n\}$ plus the constant ψ_0. We shall consider these two cases separately.

(a) Constant Potential or Constant Charge Plate. For this case, we only have one set of coefficients $\{a_n\}$ to determine. The system to be solved depends on the boundary condition on the sphere. As in the preceding section, the constant surface charge condition on the sphere is treated as a special case of linearized regulation by setting K_s, the regulation capacitance of the sphere, to 0. So we have two cases to consider: constant potential sphere and linear regulating sphere.

Constant Surface Potential Sphere. Applying the condition $\psi = \psi_s$, the constant potential on the sphere, at $r_1 = a$ and using eq 39 for a constant charge plate or 40 for a constant charge plate together with eq 43, we obtain the linear equations for $\{a_n\}$

$$(\mathbf{I} \pm \mathbf{L})\,\mathbf{a} = \psi_s \mathbf{e} - \psi_0 e^{-\kappa R}\mathbf{c} \quad (44)$$

with the appropriate choice of the constant ψ_0 as discussed above. The upper sign applies to a constant charge plate

and the lower sign to a constant potential plate. The explicit forms of the vector and matrix elements are

$$\mathbf{a}_j = a_j k_j(\kappa a) \tag{45a}$$

$$\mathbf{L}_{jn} = (2j+1)B_{nj} i_j(\kappa a)/k_n(\kappa a) \tag{45b}$$

$$\mathbf{c}_j = (2j+1) i_j(\kappa a) \tag{45c}$$

Linearized Regulating Sphere. Applying the conditions in eqs 9 and 10 at $r_1 = a$ and using eq 39 (or 40) with 43, we get

$$(\mathbf{I} \pm \mathbf{L})\mathbf{a} = \frac{aS_s}{\epsilon}\mathbf{e} - \psi_0 e^{-\kappa R}\,\mathbf{c} \tag{46}$$

where

$$\mathbf{a}_j = [(aK_s/\epsilon)k_j(\kappa a_1) - \kappa a k'_j(\kappa a)]a_j \tag{47a}$$

$$\mathbf{L}_{jn} = (2j+1)B_{nj}\frac{(aK_s/\epsilon)i_j(\kappa a) - \kappa a i'_j(\kappa a)}{(aK_s/\epsilon)k_n(\kappa a) - \kappa a k'_n(\kappa a)} \tag{47b}$$

$$\mathbf{c}_j = (2j+1)[(aK_s/\epsilon)i_j(\kappa a) - \kappa a i'_j(\kappa a)] \tag{47c}$$

and again the upper sign applies to a constant charge plate and the lower sign to a constant potential plate together with the appropriate choice for ψ_0 depending whether the plate is at constant charge or constant potential.

(b) Linearized Regulating Plate. In this case, we must not only choose the coefficients to satisfy the boundary condition on the sphere but also (9) and (10) on the plate. We first consider the simpler case $S_p = 0$ for which $\psi_0 = 0$ in the general solution given by eq 41. The more general case of $S_p \neq 0$ is covered by retaining the term $(\psi_0 e^{-\kappa z})$ with $\psi_0 = (S_p/\epsilon\kappa)$. From eq 41, with $\psi_0 = 0$, we see that the potential on the plate, $z = 0$, is

$$\psi = \sum_{n=0}^{\infty}\left\{(a_n + b_n)k_n(\kappa(R^2+\varrho^2)^{1/2})P_n\left(\frac{R}{(R^2+\varrho^2)^{1/2}}\right)\right\} \tag{48}$$

and the surface charge is given by

$$\sigma = -\epsilon\frac{\partial\psi}{\partial z}$$

$$= -\epsilon\kappa\sum_{n=0}^{\infty}\left\{\frac{(a_n - b_n)}{2n+1}\times\right.$$

$$\left[(n+1)k_{n+1}(\kappa(R^2+\varrho^2)^{1/2})P_{n+1}\left(\frac{R}{(R^2+\varrho^2)^{1/2}}\right) + \right.$$

$$\left.\left. n\,k_{n-1}(\kappa(R^2+\varrho^2)^{1/2})P_{n-1}\left(\frac{R}{(R^2+\varrho^2)^{1/2}}\right)\right]\right\} \tag{49}$$

So, substituting these results into eq 9, with $S_p = 0$, we obtain the following set of equations for $\{a_n\}$ and $\{b_n\}$

$$(1+\Delta_p)\sum_{n=0}^{\infty}\left\{(a_n + b_n)k_n(\kappa(R^2+\varrho^2)^{1/2})\times\right.$$

$$\left.P_n\left(\frac{R}{(R^2+\varrho^2)^{1/2}}\right)\right\} = (1-\Delta_p)\sum_{n=0}^{\infty}\left\{\frac{(a_n - b_n)}{2n+1}\times\right.$$

$$\left[(n+1)k_{n+1}(\kappa(R^2+\varrho^2)^{1/2})P_{n+1}\left(\frac{R}{(R^2+\varrho^2)^{1/2}}\right) + \right.$$

$$\left.\left. n\,k_{n-1}(\kappa(R^2+\varrho^2)^{1/2})P_{n-1}\left(\frac{R}{(R^2+\varrho^2)^{1/2}}\right)\right]\right\} \tag{50}$$

where $\Delta_p \equiv (K_p - \epsilon\kappa)/(K_p + \epsilon\kappa)$. Equation 50 must hold for all values of ϱ. The constant potential limit corresponds to $\Delta_p = 1$ ($K_p = \infty$) and the constant charge case corresponds to $\Delta_p = -1$ ($K_p = 0$). Unfortunately, recurrence relations derived from eq 50 connecting the coefficients $\{a_n\}$ and $\{b_n\}$ proved not to be numerically helpful. Instead we use collocation at points on the plate given by equally spaced values of the angle θ defined by $\cos\theta = R/(R^2+\varrho^2)^{1/2}$. This will give one set of equations that relates the coefficients $\{a_n\}$ and $\{b_n\}$.

The second set of equations for $\{a_n\}$ and $\{b_n\}$ comes from applying the appropriate boundary conditions on the sphere. The resulting equations differ depending whether the sphere is at constant potential or has linearized regulation boundary condition.

Constant Surface Potential Sphere. For a constant potential sphere (surface potential ψ_s), application of the boundary condition on the sphere gives

$$\mathbf{Ia} + \mathbf{Lb} = \psi_s\mathbf{e} - \psi_0 e^{-\kappa R}\,\mathbf{c} = \psi_s\,\mathbf{e} - \frac{S_p}{\epsilon\kappa}e^{-\kappa R}\,\mathbf{c} \tag{51}$$

where **a**, **L** and **c** are given by eq 45 and

$$\mathbf{b}_j = b_j k_j(\kappa a) \tag{52}$$

Linearized Regulating Sphere. For a linear regulating sphere ($\sigma = S_s - K_s\psi$), application of the boundary condition on the sphere gives

$$\mathbf{Ia} + \mathbf{Lb} = \frac{aS_s}{\epsilon}\mathbf{e} - \psi_0\,e^{-\kappa R}\,\mathbf{c} = \frac{aS_s}{\epsilon}\,\mathbf{e} - \frac{S_p}{\epsilon\kappa}e^{-\kappa R}\,\mathbf{c} \tag{53}$$

where **a**, **L**, and **c** are given by eq 47 and

$$\mathbf{b}_j = [(aK_s/\epsilon)k_j(\kappa a) - \kappa a\,k'_j(\kappa a)]b_j \tag{54}$$

This completes the specification of the linear equations that needed to be solved to obtain the coefficients in the expansion of the electrostatic potential in the electrolyte.

VI. The Force between a Sphere and a Plate

As in the unequal sphere case, we evaluate the force by integrating the total stress over the surface of the sphere. The force is then again given by eq 26 or 28, depending on the boundary condition on the sphere, but with κa replacing κa_1 and eq 22 replaced by

$$d_n(\kappa r_1) = a_n k_n(\kappa r_1) + (2n+1)i_n(\kappa r_1)\sum_{m=0}^{\infty} b_m B_{mn} + \psi_0\,e^{-\kappa R}(2n+1)i_n(\kappa r_1) \tag{55}$$

with the appropriate choice for ψ_0 depending on boundary

conditions of the plate. Of course, eq 42 should be used to simplify eq 55 for constant potential or constant charge conditions on the plate.

VII. The Interaction Free Energy between a Sphere and a Plate

As in the case of interacting spheres, the interaction free energy consists of two parts: one from a surface integration over the sphere and the other from an integration over the surface of the plate (cf. eqs 31 and 32 or 36). The contribution from the integration over the sphere has the same form as in the unequal sphere case discussed earlier. The contribution to the nondimensional interaction free energy from the sphere, U_s, is given by (34) or (38), depending on the boundary condition on the sphere, but with all subscripts changed from 1 to s (to denote the sphere). All that remains is to specify the contribution from integrating over the plate. The term proportional $\epsilon^{-\kappa z}$ in eq 39, 40, or 41 does not contribute to the interaction free energy since its contribution is independent of separation, see eqs 31 and 32 or 36.

(a) Constant Surface Potential Plate. In this case, the interaction free energy per unit area is given by (32b) so, using (42) and (49), we have for the contribution to nondimensional interaction free energy from the integration over the plate

$$U_p = 2\pi\psi_p\int_0^\infty d(\kappa\varrho)\kappa\varrho\sum_{n=0}^{\infty}\left\{\frac{a_n}{2n+1}\times\right.$$
$$\left[(n+1)k_{n+1}(\kappa(R^2+\varrho^2)^{1/2})P_{n+1}\left(\frac{R}{(R^2+\varrho^2)^{1/2}}\right)+\right.$$
$$\left.\left. n\,k_{n-1}(\kappa(R^2+\varrho^2)^{1/2})P_{n-1}\left(\frac{R}{(R^2+\varrho^2)^{1/2}}\right)\right]\right\} \quad (56)$$

In the absence of analytic expressions for these integrals, we use Gauss–Laguerre quadrature to evaluate the integrals in (46) since the integrand decays as $e^{-\kappa\varrho}$ for large $\kappa\varrho$. The potential ψ_p should be interpreted as the potential on the plate scaled by (kT/e).

(b) Linearized Regulating Plate (Including Constant Surface Charge) Plate. In this case, the contribution to the nondimensional interaction free energy from the integration over the plate is given by eq 36 and this together with the expression for the potential given by eq 48 gives

$$U_p = 2\pi\frac{\psi_0}{1-\Delta_p}\int_0^\infty d(\kappa\varrho)\times$$
$$\kappa\varrho\sum_{n=0}^{\infty}\left\{(a_n+b_n)k_n(\kappa(R^2+\varrho^2)^{1/2})P_n\left(\frac{R}{(R^2+\varrho^2)^{1/2}}\right)\right\} \quad (57)$$

where $\Delta_p \equiv (K_p - \epsilon\kappa)/(K_p + \epsilon\kappa)$ and K_p is the regulation capacity of the plate. The constant ψ_0 should be interpreted as the potential scaled by (kT/e).

The case of constant surface charge corresponds to the limit $\Delta_p = -1$, $K_p = 0$. And using (42) to eliminate $\{b_n\}$, we find the explicit expression for the contribution to dimensionless interaction free energy from a constant charge plate

$$U_p = 2\pi(e\sigma/kT\epsilon\kappa)\int_0^\infty d(\kappa\varrho)\times$$
$$\kappa\varrho\sum_{n=0}^{\infty}\left\{a_n k_n(\kappa(R^2+\varrho^2)^{1/2})P_n\left(\frac{R}{(R^2+\varrho^2)^{1/2}}\right)\right\} \quad (58)$$

Both integrals in eqs 57 and 58 are evaluated numerically by Gauss–Laguerre quadrature.

VIII. Results

For interacting dissimilar spheres or interacting sphere/plate, there are many combinations of particle sizes and boundary conditions on the two surfaces to consider. Suppose we characterize the charge state of each surface by the surface potential of each surface when they are in isolation—at a large distance ($h = \infty$) apart—we call these potentials ψ_1^{iso} and ψ_2^{iso}. We can now simplify the situation somewhat by observing that both the force and the interaction free energy in the linear Poisson–Boltzmann theory have the bilinear form

$$(\psi_1^{iso})^2 f_1(h) + \psi_1^{iso}\psi_2^{iso} f_{12}(h) + (\psi_2^{iso})^2 f_2(h)$$

where the functions $f_1(h)$, $f_{12}(h)$, and $f_2(h)$ are independent of ψ_1^{iso} and ψ_2^{iso}. Therefore it would be possible to consider just three canonical cases corresponding to the potential ratios $(\psi_1^{iso}/\psi_2^{iso}) = 1$, 0, and -1. All other combinations of ψ_1^{iso} and ψ_2^{iso} can then be constructed from the results of these three cases.

We used these three cases in order to determine the required sizes of the matrices in eqs 5, 11, 13, 44, 46, 51, and 53. For dissimilar spheres, the coefficients $\{a_n\}$ and $\{b_n\}$ are truncated at indices N_1 and N_2, respectively (the matrices are of size N_1+1 by N_2+1). As in earlier work,[10] empirically it was found that four-figure accuracy for all boundary conditions was obtained for

$$N_i = \begin{cases} 5 & \text{if } h/a_i > 1 \\ [7(a_i/h)^{1/2}] & \text{if } h/a_i < 1 \end{cases} \quad (59)$$

for $i = 1, 2$ and where $[x]$ denotes the integer part of the real number x. For the sphere/plane geometry, the coefficients $\{a_n\}$ and $\{b_n\}$ (where necessary) are both truncated at index N where, for four-figure accuracy

$$N_i = \begin{cases} 5 & \text{if } h/a > 1 \\ [6(a/h)^{1/2}] & \text{if } h/a < 1 \end{cases} \quad (60)$$

is sufficient.

In what follows, however, we will present results for four more physically useful cases having potential ratios $(\psi_1^{iso}/\psi_2^{iso})$ equal to 3, 1, -1, and -3. Since the case of identical double layers—a potential ratio of 1 with equal sizes—has been well studied,[6-11] we will pay more attention to the other cases. Since we are using the linear Poisson–Boltzmann equation, the cases with potential ratio 3 and -3 should be thought of as representing spheres with potentials of, say, 30 mV and ±10 mV.

In previous work[7,9-11] comparisons were made with the linear superposition approximation (LSA) and the Deryaguin approximation. Although the LSA has been worked out for dissimilar spheres,[3] its applicability is limited to large separations and is not considered here. The Deryaguin approximation for dissimilar spheres at constant (small) potential was first derived by Hogg, Healy, and Fuerstenau[3] and we use DA to denote the Deryaguin approximation for any boundary condition. The appropriate expression for linearized regulating surfaces has been given only recently.[8,11]

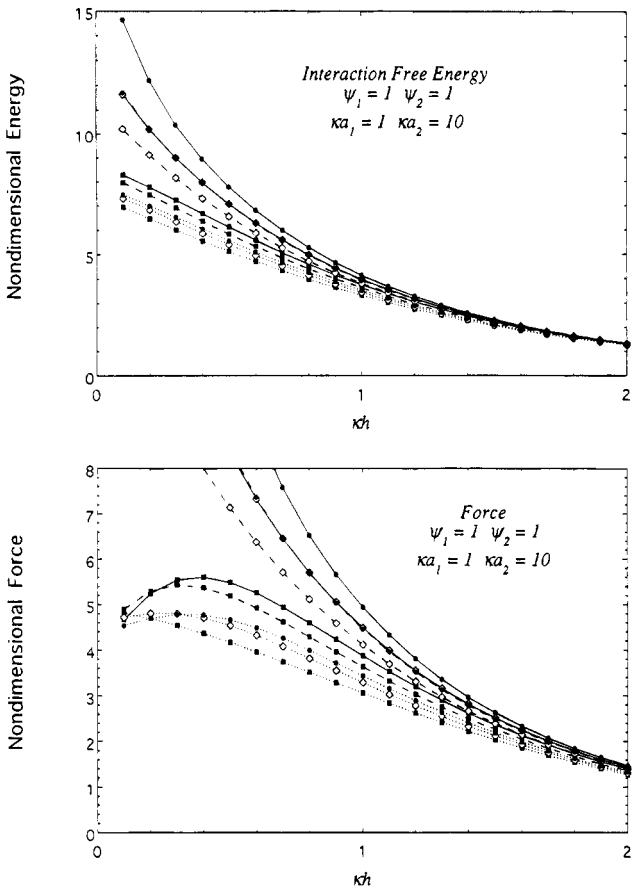

Figure 3. (a, top) Nondimensional interaction free energy, eq 35, of spheres with equal isolated potentials, $\psi_1^{iso} = \psi_2^{iso} = 1$, and unequal radii, $\kappa a_1 = 1$, $\kappa a_2 = 10$, for nine combinations of boundary conditions. The boundary condition on sphere 1 is denoted by the line style: constant charge, —; linearized regulation, – – –; constant potential, ···. The boundary condition on sphere 2 is denoted by the symbol: constant potential, ■, linearized regulation, ◇; constant charge, ●. (b, bottom) The nondimensional force, eq 25, for the same parameters as (a).

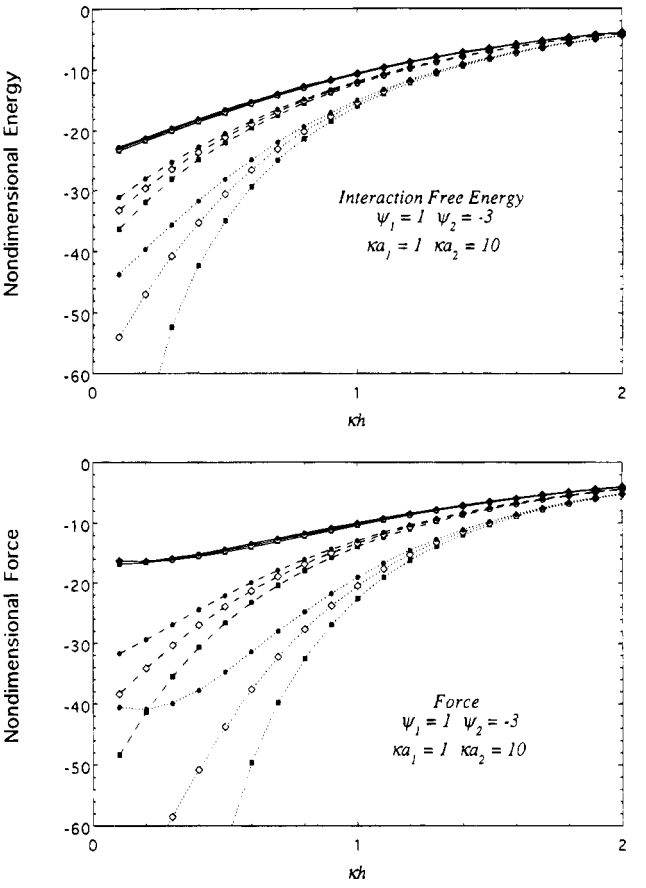

Figure 4. (a, top) Nondimensional interaction free energy of spheres with unequal isolated potentials, $\psi_1^{iso} = 1$, $\psi_2^{iso} = -3$, and unequal radii, $\kappa a_1 = 1$, $\kappa a_2 = 10$, for nine combinations of boundary conditions. Symbols and styles are as in Figure 3 so that the top three curves have sphere 1 with constant charge, the middle three curves have sphere 1 with a regulating surface, and the bottom three curves have sphere 1 with constant potential. (b, bottom) The nondimensional force for the same parameters as (a).

Deryaguin Approximation (DA).

Force (newtons):

$$f_{DA} = \frac{2\pi\epsilon\kappa a_1 a_2}{(a_1 + a_2)} \times \frac{2\psi_1^{iso}\psi_2^{iso} e^{-\kappa h} - [\Delta_1(\psi_2^{iso})^2 + \Delta_2(\psi_1^{iso})^2]e^{-2\kappa h}}{1 - \Delta_1\Delta_2 e^{-2\kappa h}} \quad (61)$$

Interaction free energy (joules):

$$u_{DA}(h) = \frac{2\pi\epsilon a_1 a_2}{(a_1 + a_2)}\left[\frac{[\Delta_1(\psi_2^{iso})^2 + \Delta_2(\psi_1^{iso})^2]}{2\Delta_1\Delta_2} \times \ln(1 - \Delta_1\Delta_2 e^{-2\kappa h}) + \frac{2\psi_1^{iso}\psi_2^{iso}}{(|\Delta_1\Delta_2|)^{1/2}} \times \begin{cases} \arctan[(-\Delta_1\Delta_2)^{1/2} e^{-\kappa h}], & (\Delta_1\Delta_2) < 0 \\ \operatorname{arctanh}[(\Delta_1\Delta_2)^{1/2} e^{-\kappa h}], & (\Delta_1\Delta_2) > 0 \end{cases}\right] \quad (62)$$

where Δ_1 and Δ_2 are defined by $\Delta_i \equiv (K_i - \epsilon\kappa)/(K_i + \epsilon\kappa)$, i = 1,2. The appropriate expressions for the sphere–plate geometry are obtained simply from eqs 61 and 62 by taking one of the radii to infinity in the prefactors.

In Figures 3 and 4 we show some results for the full range of boundary conditions covered in the previous sections. To limit the number of cases, for linearized regulating surfaces the quantity Δ_1 or Δ_2 or Δ_p is set to zero—this is the canonical "intermediate" case between constant charge and constant potential.[8] Even so, for spheres of unequal size, including a sphere and a plate, this leaves nine possible combinations of boundary conditions—each surface can be either constant potential, "intermediate", or constant charge. For spheres of equal size, degeneracies reduce this to six cases.

Figure 3 shows results pertaining to spheres of unequal size: $\kappa a_1 = 1$, $\kappa a_2 = 10$, but with equal isolated potentials—the interaction free energy in Figure 3a, the force in Figure 3b, scaled according to eqs 35 and 25, respectively. For the energy, the nine combinations of boundary conditions cover the whole range of behavior from constant charge to constant potential. That is, when both spheres are at constant charge, the repulsive interaction energy is the largest, while if both spheres are at constant potential, the repulsive energy is the smallest for all separations down to $\kappa h = 0.1$. Similarly when the spheres have equal but opposite isolated potentials (not shown), the case of both spheres at constant charge gives the least attractive interaction energy while that with both spheres at constant potential gives the most attractive interaction. Again this observation is valid for separations down to $\kappa h = 0.1$. We have not explored the behavior for smaller separations as such regions are physically less interesting. However, graphical arguments suggest that

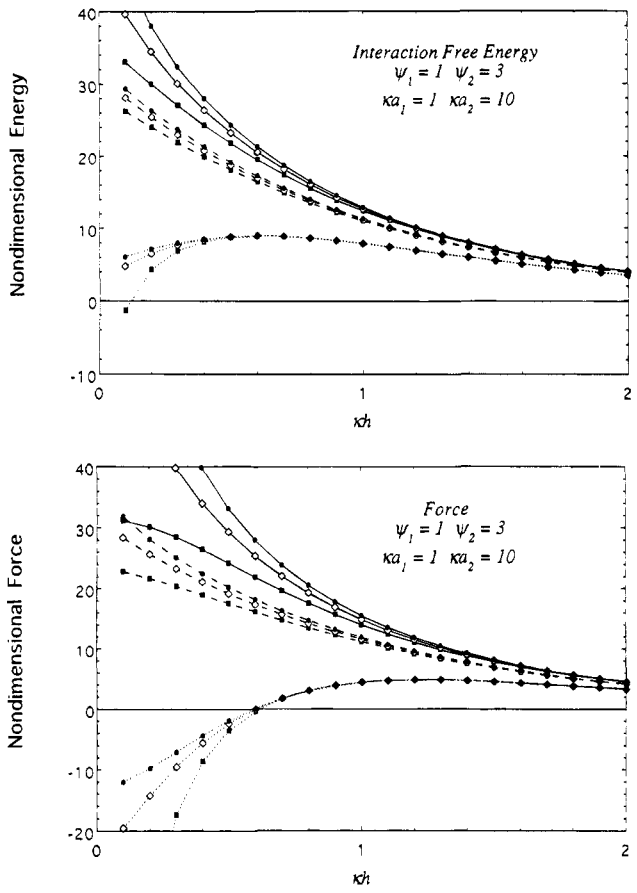

Figure 5. (a, top) Nondimensional interaction free energy of spheres with $\psi_1^{iso} = 1$, $\psi_2^{iso} = 3$ and unequal radii $\kappa a_1 = 1$, $\kappa a_2 = 10$ for nine combinations of boundary conditions. The top three curves have sphere 1 with constant charge, the middle three curves have sphere 1 with a regulating surface, and the bottom three curves have sphere 1 with constant potential. (b, bottom) The nondimensional force for the same parameters as (a).

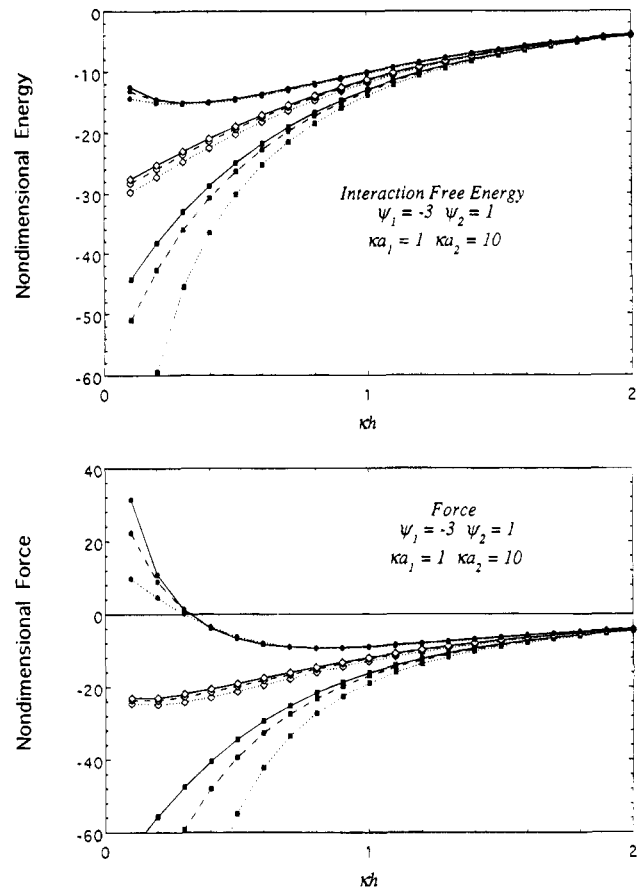

Figure 6. (a, top) Nondimensional interaction free energy of spheres with $\psi_1^{iso} = -3$, $\psi_2^{iso} = 1$ and unequal radii $\kappa a_1 = 1$, $\kappa a_2 = 10$ for nine combinations of boundary conditions. The top three curves have sphere 2 with constant charge, the middle three curves have sphere 2 with a regulating surface, and the bottom three curves have sphere 2 with constant potential. (b, bottom) The nondimensional force for the same parameters as (a).

these remarks are valid for all separations.[15,16] The same is not true for the force curves (Figure 3b) although it is violated only at separations smaller than $\kappa h \approx 0.2$. The same features are seen in recent work on interacting plates using the nonlinear Poisson–Boltzmann equation.[17] Nevertheless, the generalization that double layer interactions are bounded by the constant potential and constant charge cases is a useful approximation in most cases.

Figure 4 shows energy and force curves again for a size ratio of 10 but for a potential ratio of −3. Both sets of nine curves split into three groups of three curves except for the force at small separation. The splitting is determined by the boundary condition on the sphere with the potential of smaller magnitude (sphere 1). The bottom three curves all have constant potential boundary conditions on sphere 1, the middle three have regulation conditions on sphere 1, and the top three constant charge conditions on sphere 1. The boundary conditions on sphere 2, which has a higher value of $|\psi^{iso}|$, have a lesser effect and determine the splitting within each group of curves.

Figure 5 shows the same splitting and with the same ordering for a potential ratio of 3 and Figure 6 a splitting with different ordering for a potential ratio of −3. In Figure 6 the larger sphere (sphere 2) has the smaller value of $|\psi^{iso}|$ and so the potential on sphere 2 determines the major splitting, with the boundary condition on sphere 1 controlling the splitting within each group. Again, similar effects are seen for plates.[17]

The general conclusion is that the sphere or plate with the smaller value of $|\psi^{iso}|$ is perturbed proportionally more due to the presence of the other surface with a larger value of $|\psi^{iso}|$ and so it is the boundary condition on the sphere with the smaller value of $|\psi^{iso}|$ that primarily determines the form and magnitude of the energy or force curve. Notice that the curves become independent of boundary conditions for $\kappa h > 2$ so that effective surface potentials could be extracted from that part of the force curve. The effects of different boundary conditions are evident at smaller separation, $\kappa h < 2$.

The splitting behavior shown in Figures 3–6 for spheres of size ratio 10 is also seen for other size ratios, including a size ratio of 1, and for the sphere/plate geometry. In what follows we shall generally be content to examine only the constant charge and constant potential cases with the knowledge that other cases will exhibit behavior intermediate between these two cases.

Within the context of DLVO theory, the only approximation we are making is that of linearizing the Poisson–Boltzmann equation. It is pertinent to ask therefore, how reliable is the linear theory for given values of parameters such as κa, κh, and ψ^{iso}? In previous work,[6] we have found that for identical double layers, the linearized theory gives force curves within 10% of the nonlinear result for surface potentials up to 35–40 mV under constant potential conditions but is only qualita-

(16) Chan, D. Y. C. *J. Colloid Interface Sci.* **1983**, *95*, 193.
(17) McCormack, D.; Carnie, S. L.; Chan, D. Y. C. *J. Colloid Interface Sci.*, in press.

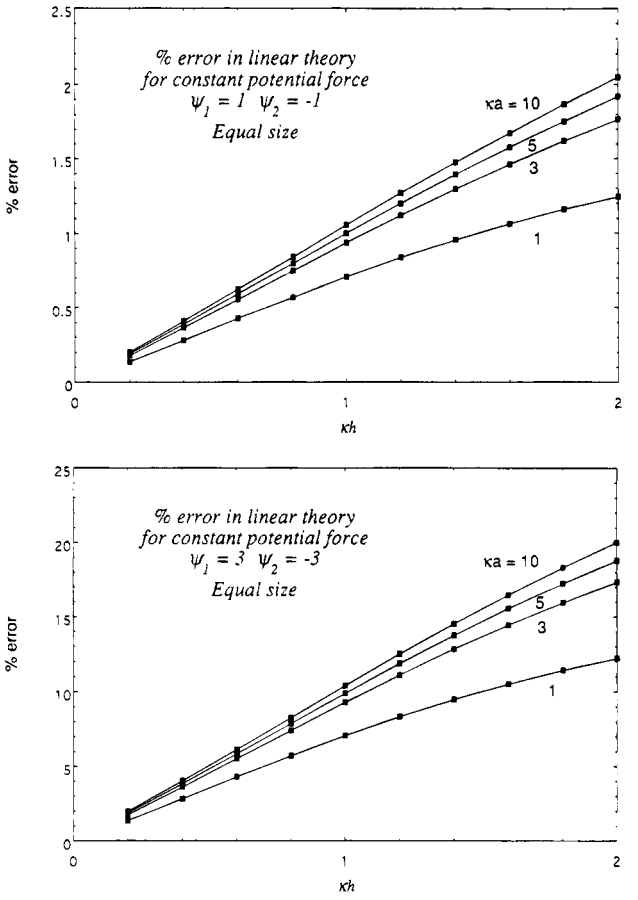

Figure 7. Percentage error in the linear theory for the force under constant potential. From top to bottom, κa = 10, 5, 3, and 1. (a, top) $\psi_1^{iso} = -\psi_2^{iso} = 1$. (b, bottom) $\psi_1^{iso} = -\psi_2^{iso} = 3$.

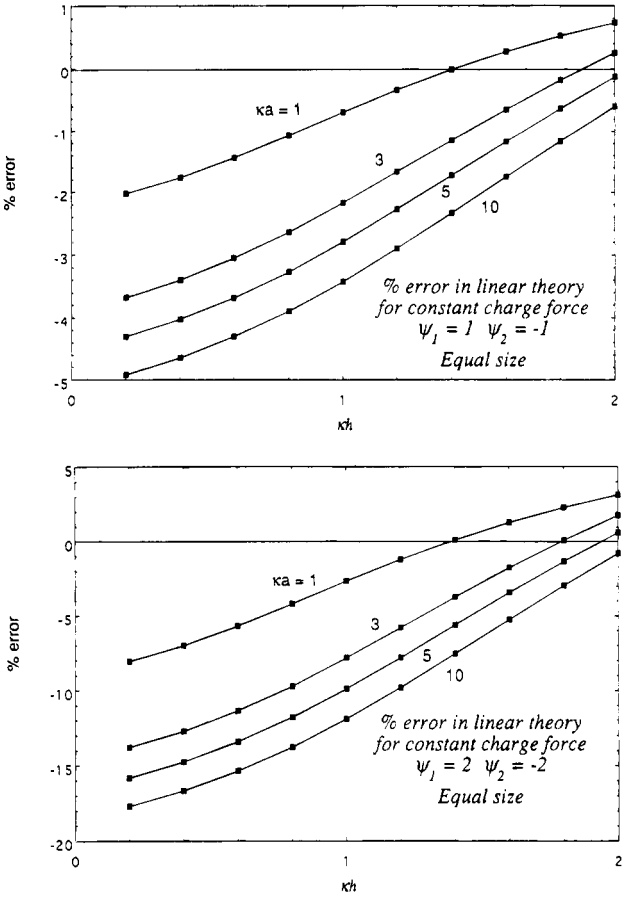

Figure 8. Percentage error in the linear theory for the force under constant charge. From top to bottom, κa = 1, 3, 5, and 10. (a, top) $\psi_1^{iso} = -\psi_2^{iso} = 1$. (b, bottom) $\psi_1^{iso} = -\psi_2^{iso} = 2$.

tively correct under constant charge conditions. However, for small particles ($\kappa a \leq 1$), the linear theory is reliable for both constant potential and constant charge boundary conditions.

For the special case of spheres of equal size and opposite isolated potentials, the force curve for the nonlinear theory can be calculated using the methods of ref 6 with two minor changes. The first is that, at the midplane, the potential vanishes rather than the radial derivative. The second difference occurs in the expression for the stress at the midplane where the osmotic pressure and transverse electric fields vanish, leaving contributions only from the radial electric fields.

For identical surfaces the performance of the linear theory can be explained by observing that in the constant potential case the potential is fixed at the boundaries and so there is relatively little freedom for the potential profile to change with surface separation. However, in the constant charge case the surface potentials rise as the spheres approach so that the linearization becomes unjustifiable. For surfaces with potentials equal in magnitude but opposite in sign, however, similar arguments would suggest that there is more room for optimism.

For surfaces having equal but opposite surface potentials interacting under constant potential, the potential is again fixed at the surfaces and as the spheres approach the potential profile varies almost linearly between the surfaces. This suggests that, provided transverse gradients are not important, the linear and nonlinear results should be close especially at small separations. For the constant charge case, the surface potentials actually fall as the spheres approach which suggests that the linear theory should get better at small separations, even for fairly large isolated potentials.

Numerical results for the nonlinear case show that these expectations are at least partially fulfilled. The ratio of linear to nonlinear results for spheres of equal size held at constant potential is shown in Figure 7 for various values of κa and ψ^{iso}. Comparison with the corresponding results in ref 6 shows that the linear theory is in fact more accurate for spheres of equal size but opposite potential than for identical spheres. The error is less than 10% even for $\kappa a = 10$ at $\psi^{iso} = 50$ mV for separation $\kappa h \leq 2$ and even for 75 mV for small separation ($\kappa h \leq 1$). In this case, our optimism has been justified. As before, the linear theory improves for smaller particles.

Results for the constant charge case for equal sized spheres are shown in Figure 8. In this case, our hopes are only partially fulfilled, in that the linear theory is very good for $\psi^{iso} = 25$ mV (error within 5% for $\kappa a = 10$) but starts to deteriorate for $\psi^{iso} = 50$ mV (error is almost 20%). Nevertheless, it is a significant improvement over the corresponding performance for identical spheres where the error varies from 25% to 150% for similar parameter values.

Having obtained exact results for the case of equal-sized spheres with opposite potentials, we can also test how the nonlinear Deryaguin approximation performs in this case. Results for the constant potential case are shown in Figure 9 and for the constant charge case in Figure 10. The nonlinear Deryaguin results are obtained by applying the Deryaguin construction to solutions of the nonlinear Poisson–Boltzmann equation for parallel plates. The results are similar to the identical sphere case[6] in that in the range $\kappa h \leq 2$ the error is within 10% provided $\kappa a \geq$

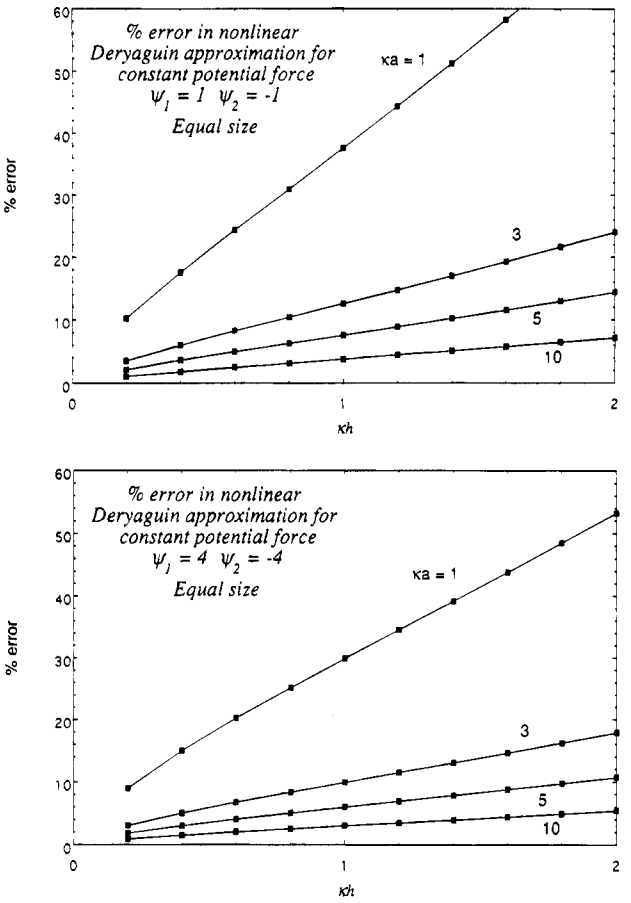

Figure 9. Percentage error in the nonlinear Deryaguin approximation for the force under constant potential. From top to bottom, $\kappa a = 1$, 3, 5, and 10. (a, top) $\psi_1^{iso} = -\psi_2^{iso} = 1$. (b, bottom) $\psi_1^{iso} = -\psi_2^{iso} = 4$.

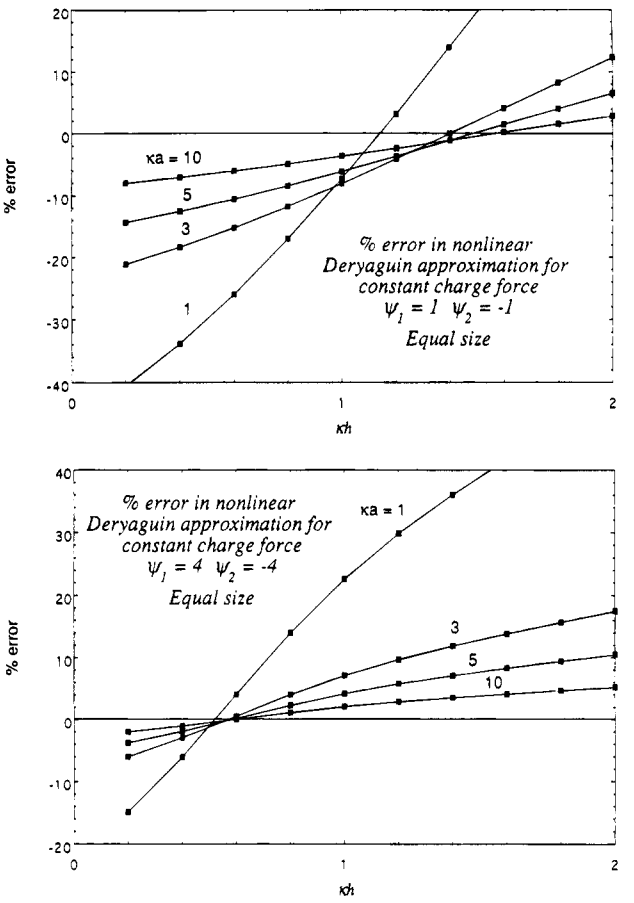

Figure 10. Percentage error in the nonlinear Deryaguin approximation for the force under constant charge. From top to bottom at $\kappa h = 2$, $\kappa a = 1$, 3, 5, and 10. (a, top) $\psi_1^{iso} = -\psi_2^{iso} = 1$. (b, bottom) $\psi_1^{iso} = -\psi_2^{iso} = 4$.

5 and improves as the isolated potential is raised. The error is similar for both constant potential and constant charge boundary conditions. It is noticeable from Figure 11a that the error in the Deryaguin result appears to scale as $(\kappa a)^{-1}$. This suggests that a correction to the Deryaguin expression to the next order in a $(\kappa a)^{-1}$ expansion should be worthwhile. Figure 11b shows the result of adding a correction of this order to the linear Deryaguin term[18,7]—although a worthwhile improvement it is clear that the correction is only valid for the regime $\kappa h \ll \kappa a$. In any case, a heruistic modification of the Deryaguin expression using Levine's surface dipole method for the constant potential case gives good accuracy for a wide range of conditions.[19]

These results, together with those of ref 6, suggest that the linear theory has a surprisingly wide region of applicability, at least for the force curves. It must be said, however, that the only evidence comes from the two rather special cases of equal-sized spheres with identical (equal but opposite) potentials. In particular, the force is always manifestly repulsive (attractive) for all boundary conditions so that none of the rich behavior seen for double layers with potentials of different magnitude (see Figures 4–6) has been directly tested. The methods of ref 6 can be extended fairly readily to those cases, which we hope to pursue in the future.

The next results we present are for the sphere/plate geometry similar to force measurements on the atomic force microscope. For this reason we limit ourselves to force curves in this section. In this geometry there is only one value of κa, and by varying this parameter, we study the effect of the curvature of the spherical particle. In Figure 12 we show results for $\kappa a = 10$ where a priori we would expect the Deryaguin approximation to perform well. For the comparison in Figure 12, the Deryaguin result is given by eq 61, which is obtained by applying the Deryaguin construction to the linearized Poisson–Boltzmann result for parallel plates[8]—we call this the linear Deryaguin approximation. For the cases where both surfaces have constant potential or are regulating, the accuracy of the linear Deryaguin approximation is confirmed by the data. However the constant charge case is never accurate for $\kappa h < 1$ with the exception of the case with potential ratio equal to −1. This special case is the only case where the linear Deryaguin approximation gives a force that is always attractive—in every other case, the constant charge curve becomes repulsive at sufficiently small separation. Similarly, the linear Deryaguin approximation for the constant potential case is always repulsive only for identical surfaces—it becomes attractive for sufficiently small separation in all other cases. However, the linear Deryaguin approximation is good for constant potential surfaces even in these attractive cases.

The effect of the particle curvature can be seen in Figure 13 where, in one case, the sphere has the potential of lower magnitude (Figure 13a) and, in the other, it is the plate (Figure 13b). Since it is the surface of lower (in magnitude) potential that controls the interaction, as in the splitting seen in Figures 3–5, the linear Deryaguin approximation is noticeably worse in describing the first

(18) Ohshima, H.; Chan, D. Y. C.; Healy, T. W.; White, L. R. *J. Colloid Interface Sci.* **1983**, *92*, 232.
(19) Sader, J.; Chan, D. Y. C.; Carnie, S. L. To be submitted for publication.

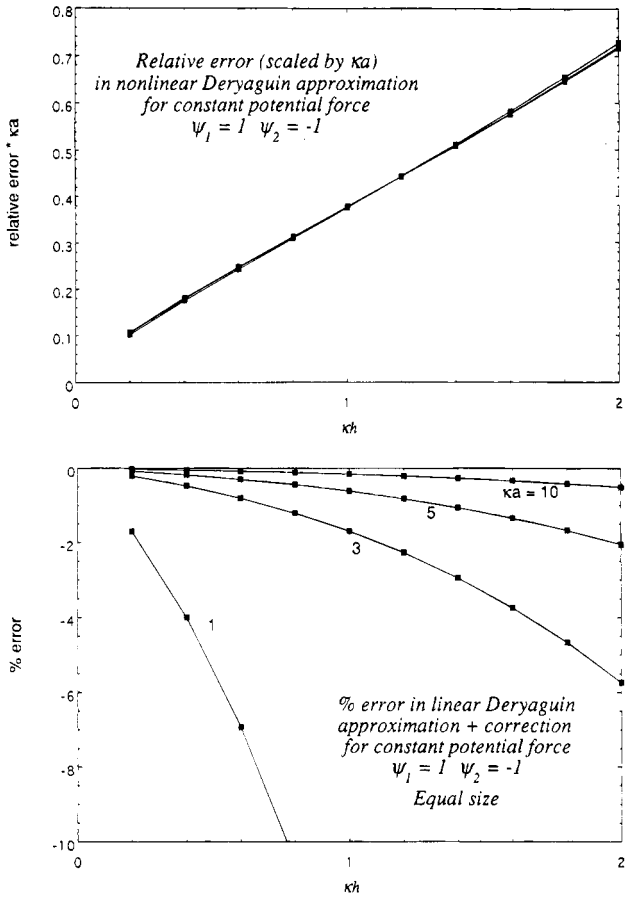

Figure 11. (a, top) Error in the force from the nonlinear Deryaguin approximation under constant potential multiplied by κa, for $\kappa a = 1$, 3, 5, 10 and $\psi_1^{iso} = -\psi_1^{iso} = 1$. (b, bottom) The percentage error in the corrected force (the linear Deryaguin force plus the correction from ref 18) compared to the linear theory under constant potential for $\psi_1^{iso} = -\psi_2^{iso} = 1$. From top to bottom, $\kappa a = 10$, 5, 3, and 1.

case, where the important surface has $\kappa a = 10$, than the second case. Nevertheless, the performance is good except for constant charge surfaces.

Figure 14 shows similar results for a sphere with $\kappa a = 1$. As expected, the linear Deryaguin approximation performs worse for such a small particle but there are several notable features of the curves. Firstly, the constant potential and regulating cases are still described remarkably well. It is as if having one surface as a plate with infinite radius of curvature has extended the applicability of the linear Deryaguin approximation to low values of κa. A heuristic explanation of this observation is given in ref 19. Secondly, the constant charge results are again good only for a potential ratio equal to -1; all other cases are poorly handled. In particular, the behavior for a potential ratio of -3 is not even qualitatively correct at $\kappa a = 1$ with the Deryaguin approximation giving quite strong repulsion compared to a mild attraction in the exact calculation.

In the case of regulating surfaces with $\Delta_s = \Delta_p = 0$, the linear Deryaguin approximation reduces to the linear superposition approximation[8]—this may explain the relatively good performance for this case for a wide variety of conditions.

In Figures 15 and 16 we show results for "mixed" boundary conditions—one surface has constant charge and the other constant potential. Again, the performance is remarkably good at $\kappa a = 10$ and deteriorates somewhat at $\kappa a = 1$. Once again the surface with the lower (in magnitude) potential controls the interaction so, if it has

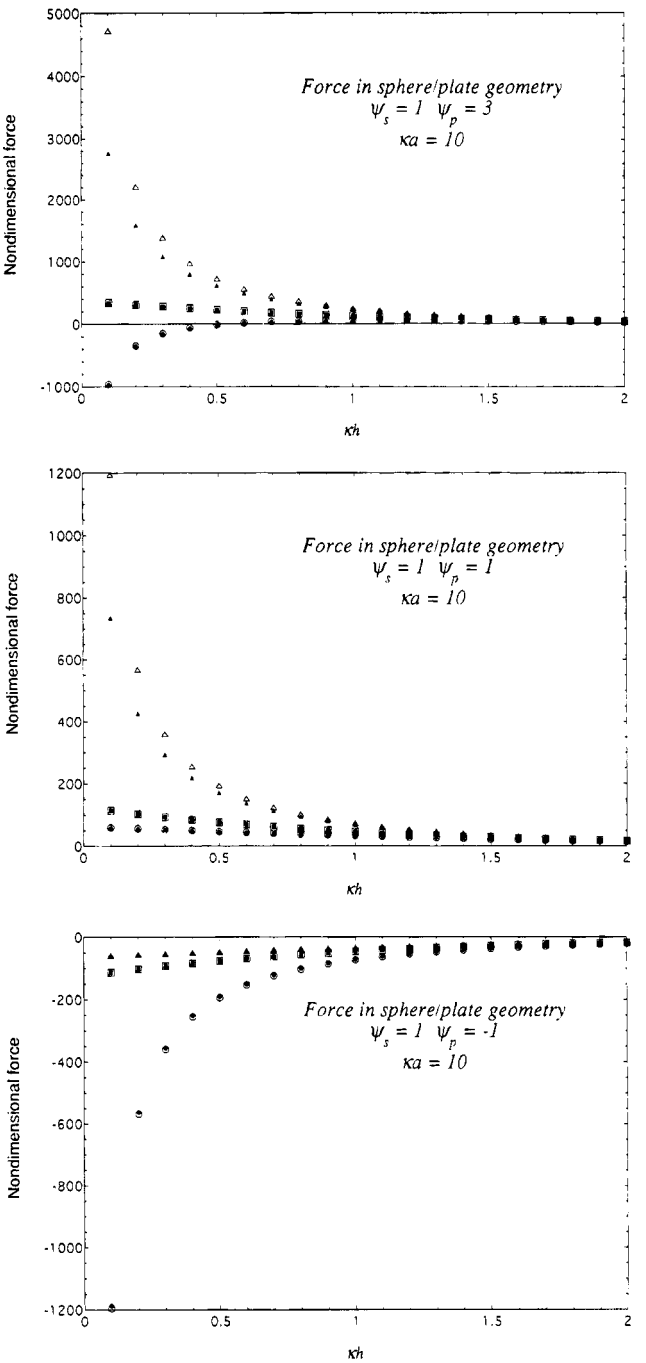

Figure 12. Force curves in the sphere/plate geometry for $\kappa a = 10$ and three sets of boundary conditions: from top to bottom, both surfaces constant charge, both surfaces regulating, both surfaces constant potential. Results of the linear theory are shown as small solid symbols, corresponding results for the linear Deryaguin approximation are shown as large open symbols. (a, top) $\psi_s^{iso} = 1$, $\psi_p^{iso} = 3$. (b, middle) $\psi_s^{iso} = 1$, $\psi_p^{iso} = 1$. (c, bottom) $\psi_s^{iso} = 1$, $\psi_p^{iso} = -1$.

constant potential, the curve is "constant-potential-like" e.g. the lower pair of curves in Figure 15, corresponding to the sphere in parts a and b of Figure 15 and the plate in Figure 15c. Again, by far the worst performance is for a "constant-charge-like" curve with potential ratio equal to -3 at low κa (Figure 16b).

To summarize, the sphere/plate geometry has the happy result of extending the applicability of the linear Deryaguin approximation to values of κa as low as perhaps 1 but certainly 3 for any boundary conditions except constant charge. In that case, it consistently overestimates the force except for a potential ratio equal to -1. For a potential ratio of -3 at low κa, the linear Deryaguin

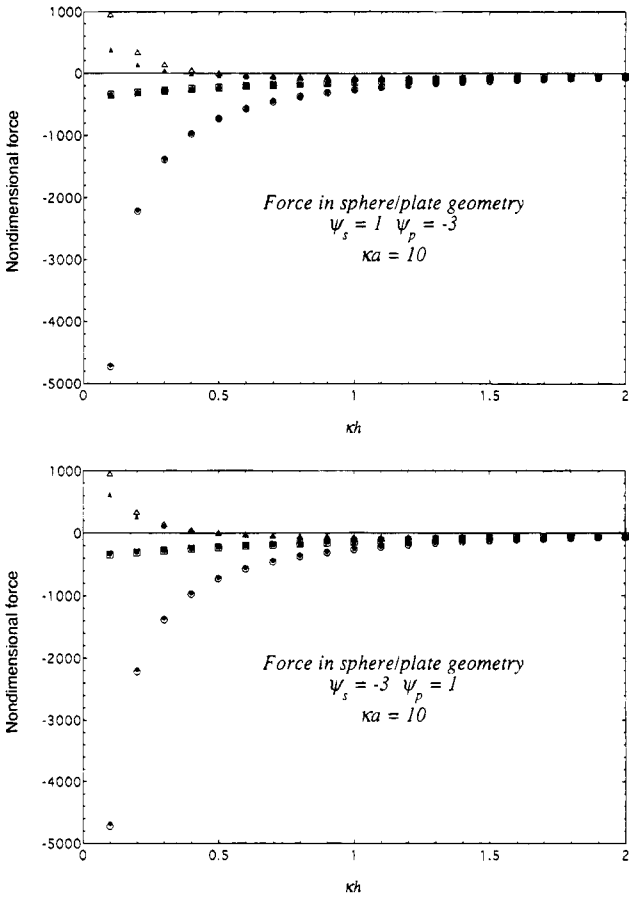

Figure 13. As for Figure 12 but with (a, top) $\psi_s^{iso} = 1$, $\psi_p^{iso} = -3$ and (b, bottom) $\psi_s^{iso} = -3$, $\psi_p^{iso} = 1$.

approximation is qualitatively wrong. Our confidence in this statement is bolstered by the good performance of the linear theory at low κa compared to the nonlinear theory as we have seen here and in ref 6.

Having dealt so exhaustively with the sphere/plate geometry it is only necessary to mention the new features exhibited by dissimilar spheres. Because heterocoagulation studies (for example, ref 11) tend to focus on the interaction energy, we will present the interaction free energy curves in what follows.

With both surfaces now being of colloidal dimension, we would expect the Deryaguin approximation to be less accurate than in the above discussion. In Figures 17 and 18 we show results for spheres of equal size. The energy curves at $\kappa a = 10$ show all the characteristics of the force curves above: good performance for constant potential but not for constant charge, except at a potential ratio of -1. At $\kappa a = 1$ the agreement is much worse in terms of the relative error especially at large κh—a feature that does not show up in the force curves above. A key ingredient in improving the performance of the Deryaguin approximation for the energy is to incorporate the correct asymptotic behavior at large κh.[19]

By comparing Figure 18 against Figures 19 and 20, we see the effect of increasing the size ratio of the particles from 1 to 5 to infinity with one particle held at $\kappa a = 1$. The performance of the Deryaguin approximation in the range $1 \leq \kappa h \leq 2$ improves in all cases. The constant charge case is never very accurate and the constant potential curve at a potential ratio of -3 improves dramatically. The performance of the constant potential curve at a potential ratio of 3 is more problematic—it appears that the agreement at $\kappa a_1 = \kappa a_2 = 1$ may be fortuitous.

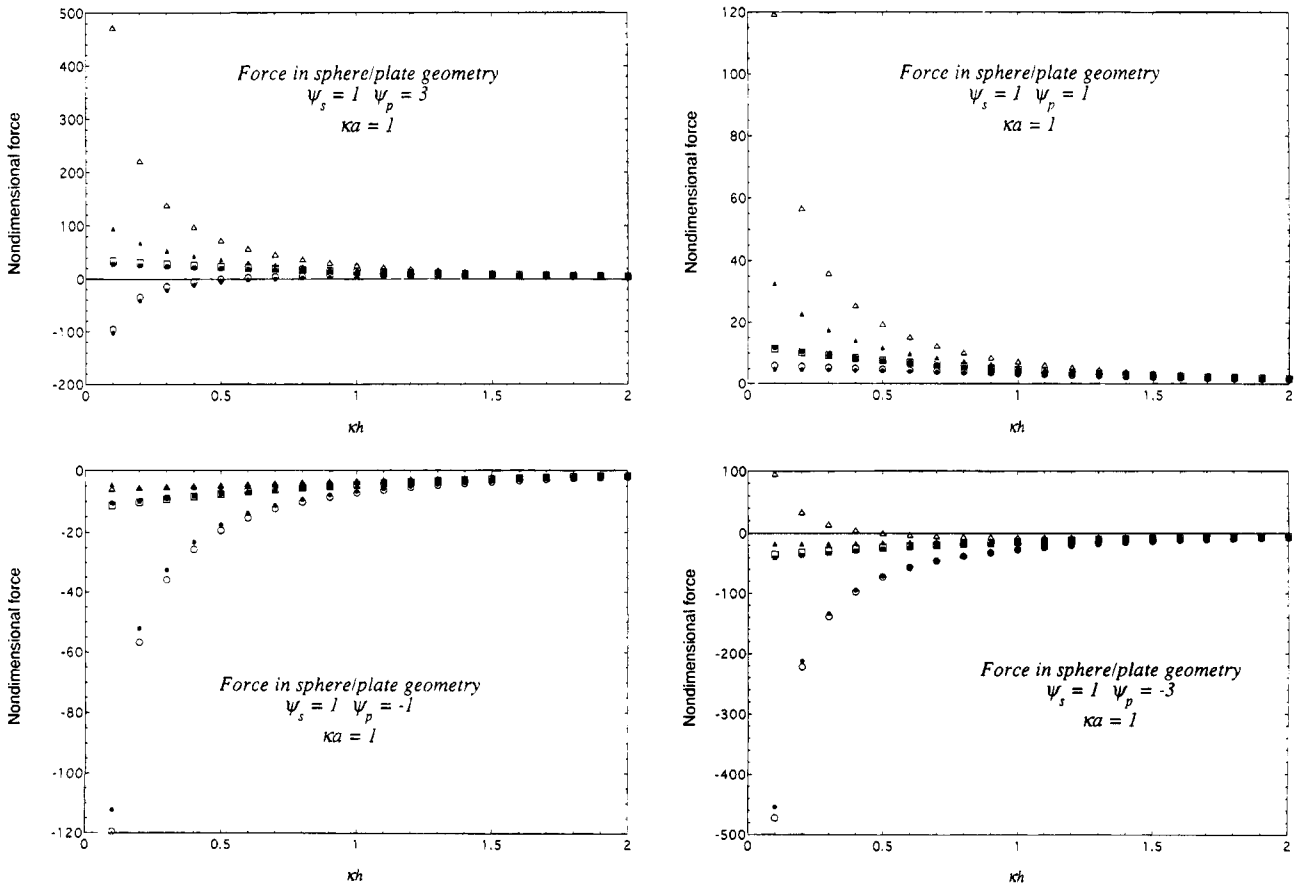

Figure 14. As for Figure 12 but with $\kappa a = 1$ and (a, top left) $\psi_s^{iso} = 1$, $\psi_p^{iso} = 3$, (b, top right) $\psi_s^{iso} = 1$, $\psi_p^{iso} = 1$, (c, bottom left) $\psi_s^{iso} = 1$, $\psi_p^{iso} = -1$, and (d, bottom right) $\psi_s^{iso} = 1$, $\psi_p^{iso} = -3$.

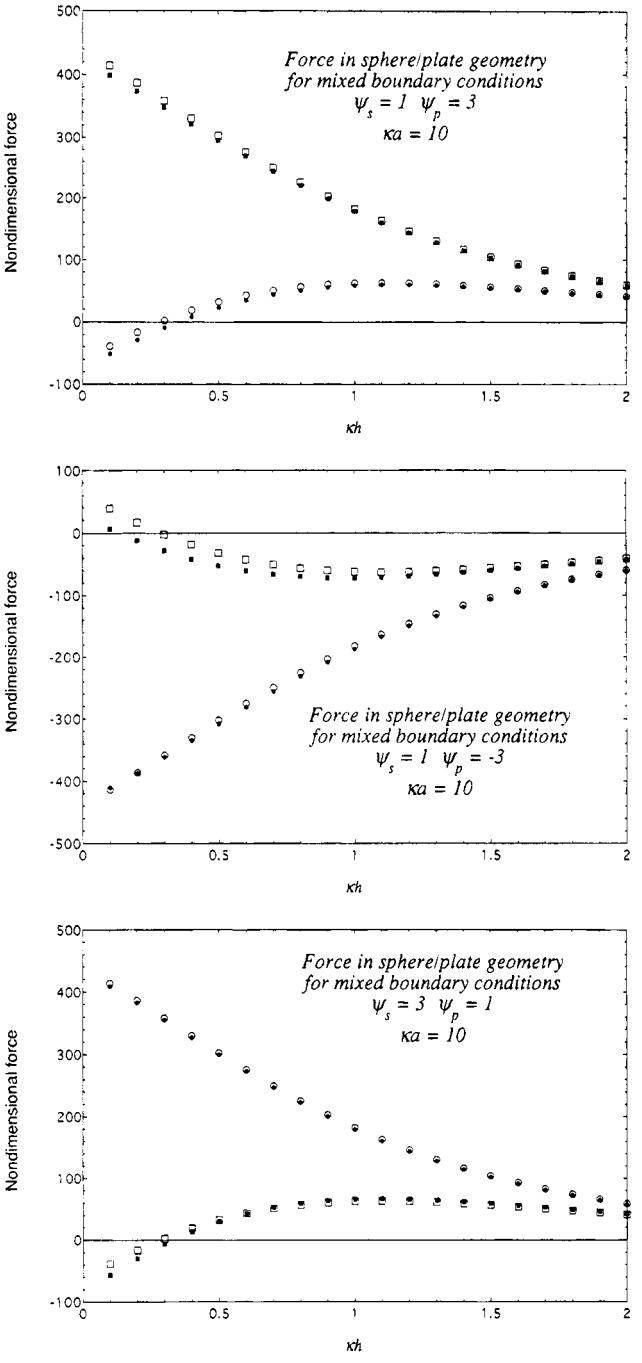

Figure 15. Force curves in the sphere/plate geometry for $\kappa a = 10$ and two sets of "mixed" boundary conditions: circles denote the case of a constant charge plate and a constant potential sphere, squares denote the case of a constant potential plate and a constant charge sphere. As before, results of the linear theory are shown as small solid symbols and corresponding results for the linear Deryaguin approximation are shown as large open symbols. (a, top) $\psi_s^{iso} = 1$, $\psi_p^{iso} = 3$. (b, middle) $\psi_s^{iso} = 1$, $\psi_p^{iso} = -3$. (c, bottom) $\psi_s^{iso} = 3$, $\psi_p^{iso} = 1$.

IX. Conclusions

We have shown how to obtain solutions for the double layer force and interaction free energy for dissimilar colloidal spheres as well as between a sphere and a plate, according to the linearized Poisson–Boltzmann equation. Numerical calculations here and in ref 6 suggest that such results are reasonable, especially for constant potential surfaces, for surface potentials approaching 40 mV.

For experimentalists using the atomic force microscope, the most significant finding is that, except if the surfaces

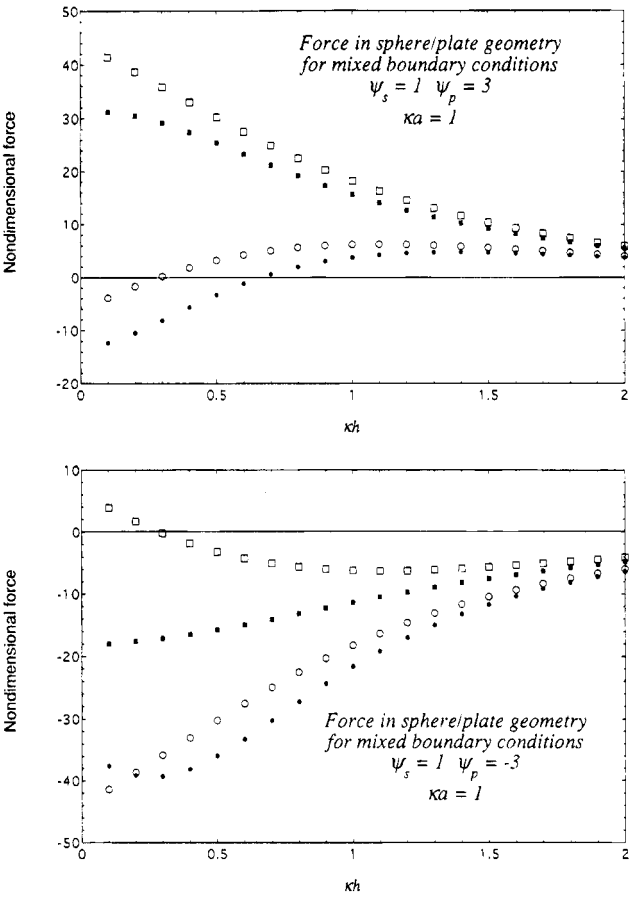

Figure 16. As for Figure 15 but with $\kappa a = 1$. (a, top) $\psi_s^{iso} = 1$, $\psi_p^{iso} = 3$. (b, bottom) $\psi_s^{iso} = 1$, $\psi_p^{iso} = -3$.

under study are known to be constant charge surfaces, the Deryaguin approximation gives an accurate picture of the double layer force between a sphere and a plate for particle sizes currently used in the AFM. Since results from the nonlinear Poisson–Boltzmann equation[6] show that the Deryaguin approximation improves at higher potentials, this strongly suggests that the Deryaguin approximation should be adequate for the analysis of sphere/plate force curves in most circumstances. Even in the constant charge case, the Deryaguin approximation consistently provides an upper bound on the true force.

For heterocoagulation studies, the picture is similar except that the energy curves start to deteriorate once both particle sizes fall below $\kappa a = 5$. For very small precursor particles ($\kappa a < 1$) the linearized Poisson–Boltzmann equation is known to be good[6] and so the present method should be reliable. This method is not numerically daunting—each force or energy curve presented here only takes at most a few minutes to calculate on a Macintosh Centris 650.

Needless to say, the comparatively good performance of the Deryaguin approximation compared to an exact solution of the linearized Poisson–Boltzmann equation found here for particles of quite different size and isolated surface potentials is in marked contrast to the claimed poor performance by Barouch et al.[20] The theoretical flaws in that work have been eloquently stated by Overbeek[21]—it suffices to say here that our numerical calculations support the arguments of Overbeek in every respect.

(20) Barouch, E.; Matijevic, E.; Ring, T. A.; Finlan, J. M. *J. Colloid Interface Sci.* **1978**, *67*, 1, and later papers cited in ref 21.
(21) Overbeek, J. Th. *J. Chem. Soc., Faraday Trans. 1* **1988**, *84*, 3079.

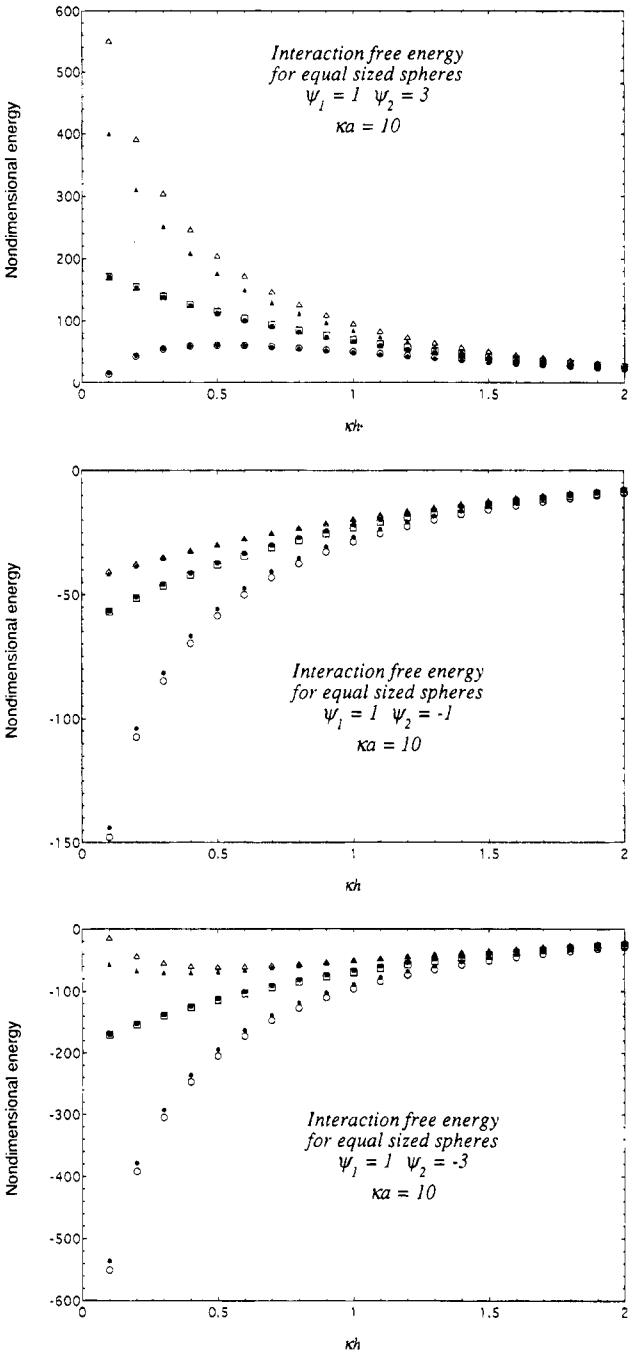

Figure 17. Interaction free energy curves for spheres of equal size $\kappa a_1 = \kappa a_2 = 10$ and three sets of boundary conditions, from top to bottom, both surfaces constant charge, both surfaces regulating, both surfaces constant potential. Results of the linear theory are shown as small solid symbols; corresponding results for the linear Deryaguin approximation are shown as large open symbols. (a, top) $\psi_1^{iso} = 1$, $\psi_2^{iso} = 3$. (b, middle) $\psi_1^{iso} = 1$, $\psi_2^{iso} = -1$. (c, bottom) $\psi_1^{iso} = 1$, $\psi_2^{iso} = -3$.

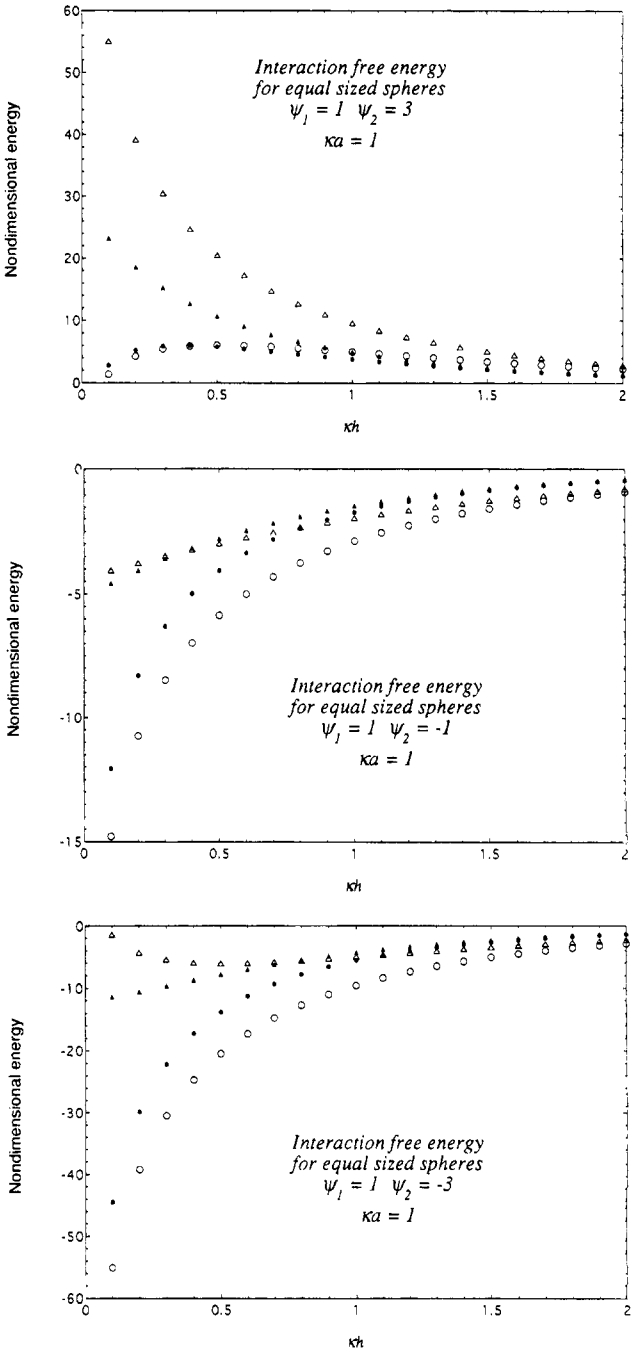

Figure 18. As for Figure 17 but with $\kappa a_1 = \kappa a_2 = 1$ and two sets of boundary conditions, from top to bottom, both surfaces constant charge, both surfaces constant potential. (a, top) $\psi_1^{iso} = 1$, $\psi_2^{iso} = 3$. (b, middle) $\psi_1^{iso} = 1$, $\psi_2^{iso} = -1$. (c, bottom) $\psi_1^{iso} = 1$, $\psi_2^{iso} = -3$.

The one remaining doubt in this work is how reliable are these conclusions for particles with large surface potentials. In two special cases, equal size spheres with equal or opposite surface potentials, we have answered those doubts. Those results strongly suggest that the Deryaguin approximation improves at large surface potentials and so the general conclusions regarding the effects of size ratio and curvature are correct. Definitive evidence however awaits numerical results of the nonlinear Poisson–Boltzmann equation for dissimilar spheres and the sphere/plate geometry, a goal we now believe is in sight.

Glossary

a_1, a_2	sphere radii
a_n, b_n	coefficients in the two center expansion of the potential
S, K	parameters for the linearized regulation model
f	force in newtons
F	$=f(h)/(\epsilon(kT/e)^2)$ nondimensional force
h	shortest distance between the spheres or between sphere and plate
U	$=u(h)/(\epsilon(kT/e)^2\kappa^{-1})$ nondimensional interaction free energy
u	interaction free energy in joules

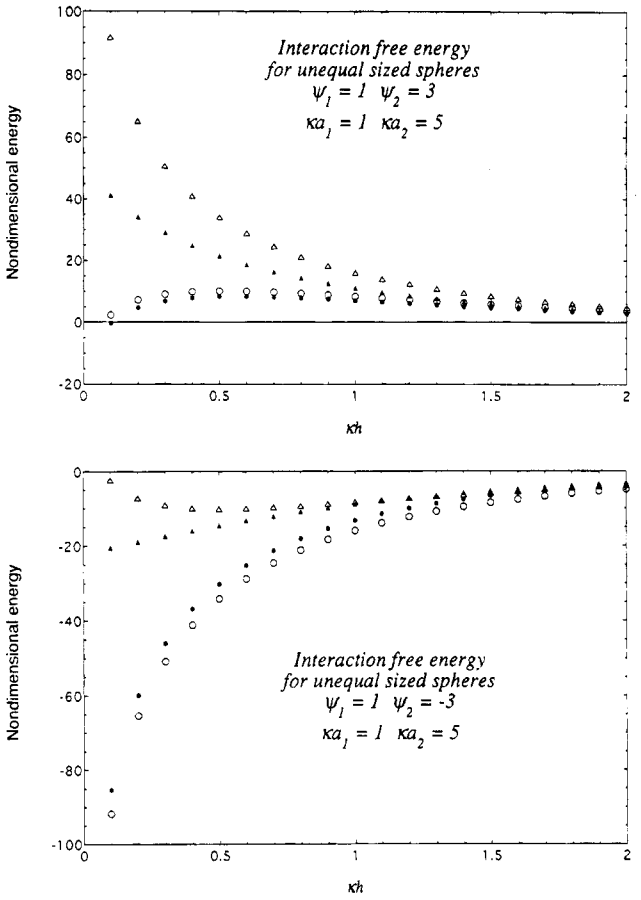

Figure 19. As for Figure 18 but for spheres of unequal size $\kappa a_1 = 1$, $\kappa a_2 = 5$. (a, top) $\psi_1^{iso} = 1$, $\psi_2^{iso} = 3$. (b, bottom) $\psi_1^{iso} = 1$, $\psi_2^{iso} = -3$.

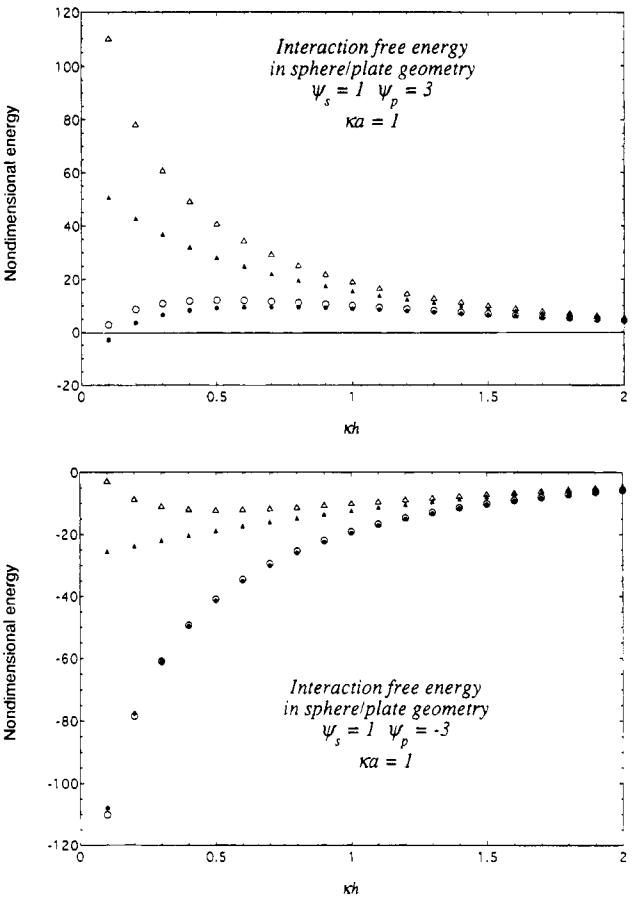

Figure 20. As for Figure 18 but with a sphere ($\kappa a = 1$) and a plate. (a, top) $\psi_s^{iso} = 1$, $\psi_p^{iso} = 3$. (b, bottom) $\psi_s^{iso} = 1$, $\psi_p^{iso} = -3$.

ϵ, ϵ_p	$\epsilon_0\epsilon_r$, $\epsilon_0\epsilon_{rp}$ = product of the permittivity of vacuum and the relative permittivity of the solvent (water), ϵ_r, or the particle, ϵ_{rp}
κ	Debye screening parameter
ψ	surface potential of a sphere in isolation
σ	surface charge density of a sphere in isolation, C/m^2

Acknowledgment. This work is supported in part by the Advanced Mineral Processing Centre, a Special Research Centre funded by the Australian Federal Government at the University of Melbourne. Support by the Australian Research Council to S.L.C. and D.Y.C. is gratefully acknowledged.